


Research Article

New insights into the glacial and relative sea-level history of the western Fraser Lowland based on sediment cores from geotechnical drilling for the Evergreen Tunnel, British Columbia, Canada

Lionel E. Jackson^a , Brent C. Ward^a, Stephen R. Hicock^b, Raphael Gromig^a, John J. Clague^a and Derek G. Turner^c

^aDepartment of Earth Sciences, Simon Fraser University, Burnaby, British Columbia V5A 1S6, Canada; ^bDepartment of Earth Sciences, Western University, London, Ontario N6A 5B7, Canada and ^cEarth and Environmental Science, Douglas College, New Westminster, British Columbia V3M 5Z5, Canada

Abstract

Geotechnical drilling for a tunnel between Port Moody and Burnaby, BC, Canada, uncovered a buried fjord. Its sedimentary fill has a thickness of at least 130 m and extends more than 37 m below present mean sea level. Recovered sediments record cyclical growth and decay of successive Cordilleran ice sheets. The oldest sediments comprise 58 m of almost stoneless silt conformably overlying ice-proximal sediments and till, which in turn overlie bedrock. These sediments may predate Marine Isotope Stage (MIS) 4. Glacial sediments assigned to MIS 4 overlie this basal succession and, in turn, are overlain by MIS 3 interstadial sediments and sediments from two MIS 2 glacial advances. Indicators of relative sea-level elevations that bracket glacial deposits of MIS 4 and 2 indicate the cyclic existence of moat-like isostatic depressions in the front of expanding ice sheets. Compared with present sea level, these depressions were at least 160 m during the onsets of MIS 4 and MIS 2. Assuming a maximum eustatic drawdown of 120 m during MIS 2, isostatic depression may have exceeded 200 m during retreat of glacial ice from the Evergreen tunnel area. This is consistent with region-specific low mantle viscosity and rapid Cordilleran Ice Sheet buildup and wasting.

Keywords: Relative sea level, Fraser Lowland, Cordilleran Ice Sheet, Glaciation, Sediment cores, Fraser glaciation, Till, Glaciotectonism

(Received 18 April 2023; accepted 19 January 2024)

Introduction

British Columbia (BC, Canada; Fig. 1) has been repeatedly affected by successive ice sheets (e.g., Clague and James, 2002; Booth et al., 2003) (for clarity, only the last is referred to as the “Cordilleran Ice Sheet” in this paper (Clague, 1989). The record of the middle and late Pleistocene glaciation of southwest British Columbia has been pieced together from various fragmental and typically limited natural exposures and excavations (e.g., Hicock, 1976; Hicock and Lian, 1999). However, recent infrastructure development has enabled refinement of this record. Between 2000 and 2015, geotechnical drilling was conducted in advance and during construction of the 10.9-km-long Evergreen Extension to the Millennium Line of the Greater Vancouver area light rail transit system, Skytrain (Fig. 1). Its construction required driving a 2.2-km-long, roughly north-south oriented tunnel beneath a topographic saddle between Burnaby Mountain (summit elevation 370 m above sea level (m asl) and the Chines in Coquitlam (elevation ~160 m asl). These uplands are underlain by south-dipping Eocene-age clastic rocks

(Huntingdon Group) and covered by a veneer of glacial drift from Marine Isotope Stage (MIS) 2 (Armstrong and Hicock, 1976; Mustard and Rouse, 1994). However, rather than encountering a bedrock saddle between these uplands, drilling revealed a 4-km-long, north-south oriented buried fjord infilled with glacial and nonglacial sediments (Golder Associates, 2010).

The large accommodation space of this buried fjord (informally called “Evergreen fjord”) provides a nearly continuous record of perhaps the last 160,000 yr that allowed testing of glacial models and estimation of glacially isostatic-driven relative sea-level changes. This is the most complete record of glacial and nonglacial sediments of any single location in the Greater Vancouver area. It indicates four incursions of glacial ice and significant glacio-isostatic depression and glacio-isostatically driven relative sea-level changes. Furthermore, these sediments will be available for future study through drilling after sand and gravel pits and other ephemeral exposures, which constitute much of the glacial record in the Greater Vancouver area, are gone, underlining the significance of this sedimentary archive.

Stratigraphic framework

Stratigraphic studies of glacial sediments in the Fraser Lowland of British Columbia (Fig. 1) were initiated in earnest by J.E. Armstrong and colleagues in the late 1940s (Armstrong, 1953;

Corresponding author: Brent C. Ward; Email: bcward@sfu.ca

Cite this article: Jackson LE, Ward BC, Hicock SR, Gromig R, Clague JJ, Turner DG (2024). New insights into the glacial and relative sea-level history of the western Fraser Lowland based on sediment cores from geotechnical drilling for the Evergreen Tunnel, British Columbia, Canada. *Quaternary Research* 1–22. <https://doi.org/10.1017/qua.2024.9>

© The Author(s), 2024. Published by Cambridge University Press on behalf of Quaternary Research Center. This is an Open Access article, distributed under the terms of the Creative Commons Attribution licence (<http://creativecommons.org/licenses/by/4.0/>), which permits unrestricted re-use, distribution and reproduction, provided the original article is properly cited.



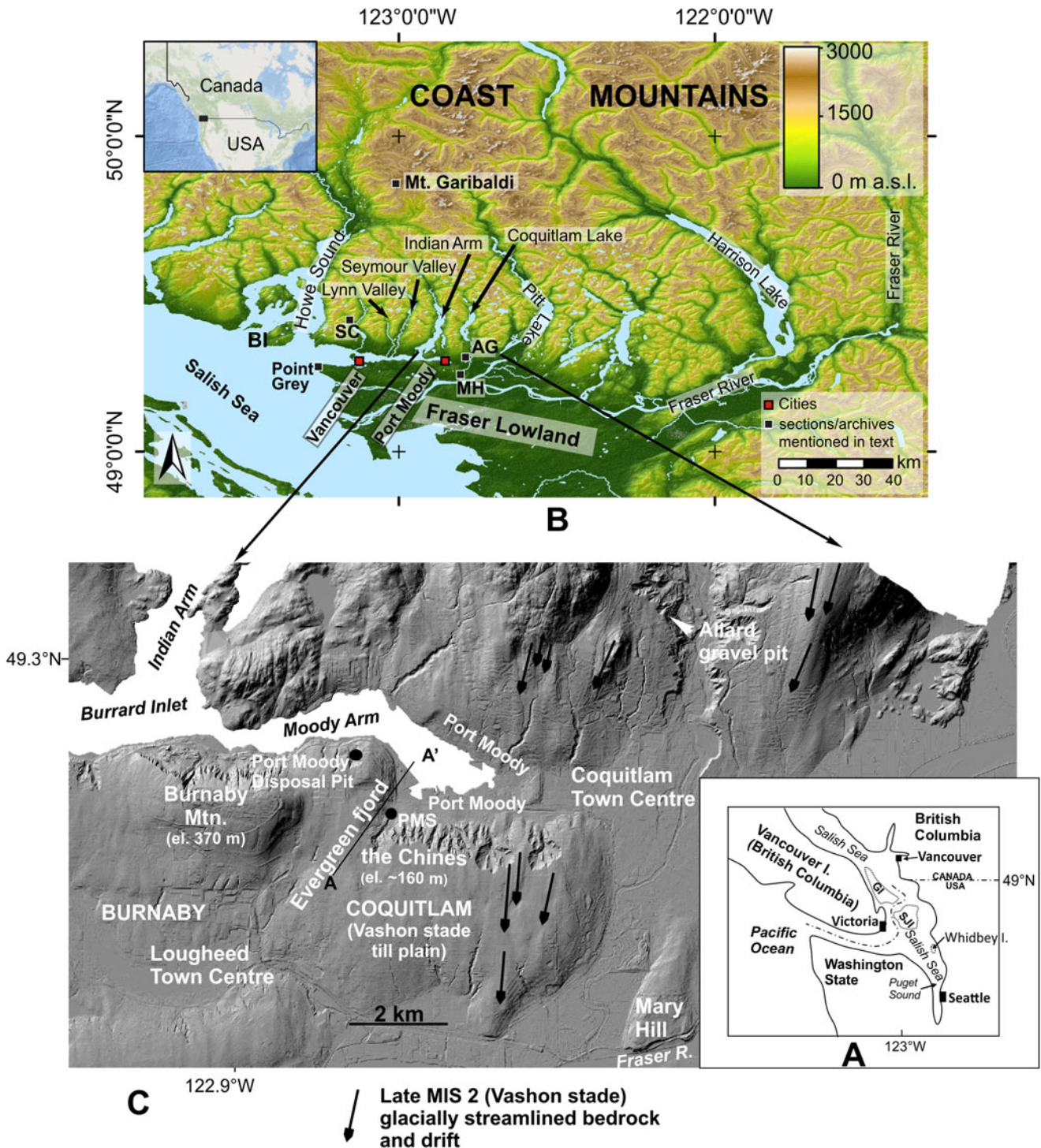


Figure 1. Location of study area. (A) Southwest British Columbia and northwest Washington State: SJI, San Juan Islands (USA); GI, Gulf Islands (Canada). (B) Greater Vancouver area includes the cities of Vancouver, Burnaby, and Coquitlam and is located in the western part of the Fraser Lowland, which is part of the larger Georgia Depression (largely infilled by the Salish Sea). BI, Bowen Island; MH, Mary Hill; SC, Sisters Creek; AG, Allard gravel pit. (C) LIDAR image of the Vancouver area, including the site of the Evergreen rapid transit line. A-A': line of profile and boreholes.

Armstrong and Brown, 1953). By the mid-1950s, they recognized that the Fraser Lowland, including the Greater Vancouver area, is underlain by a succession of buried landscapes separated by erosional unconformities. Each package contains glacial sediments from glacial advances along with nonglacial, organic-rich sediments (Clague, 1985; Clague and Ward, 2011).

Advance phases, based on evidence from the Cordilleran Ice Sheet of the MIS 2-age Fraser glaciation (correlative to Late Wisconsin glaciation; Fig. 2), were marked by glacio-isostatic depression (Clague *et al.*, 2005). Total depression during full glacial loading is estimated to be in the 400 to 500 m range relative to present sea level. Glacio-isostatic rebound that followed glacial retreat

Geologic event-units and lithostratigraphy of previous studies¹

Geologic/ MIS time scales (k cal. years)	Geologic-event units		¹⁴ C age (ka BP)	Lithostratigraphic units				
	Georgia Dep.	N. Van. to Coquitlam		Northern Puget lowland/ Whidbey I. (Easterbrook 1994; Porter 2011)	Southeast Vancouver I. ¹ (Alley and Hicock 1986 Lian et al. 1995)	Vancouver ² (Armstrong 1975; Armstrong and Hicock 1979; Clague 1977; Clague et al. 2005)	N. Vancouver (Capilano, Lynn, Seymour basins) (Hebda et al. 2016; Hicock and Lian 1995, 1999)	Coquitlam/ Port Moody (Hicock and Armstrong 1981; Hicock and Lian 1999)
HOLOCENE	Postglacial					Salish sediments	Salish sediments	Salish sediments
MIS 1			5					
14.7			10					
	Glaciation (late)	Fraser Glaciation	11	Fraser	Fraser	Capilano seds.	Capilano seds.	Capilano seds.
			14					
		Vashon Stade	14			Vashon till	Vashon Drift	Vashon Drift
MIS 2		Port Moody Interstade	18	Drift (includes the Esperance Sand member: equivalent to Quadra Sand)	Glacial	Quadra Sand	Sisters Ck. Fm.	Quadra Sand Sisters Ck. Fm.
29		Coquitlam Stade	22		deposits (Quadra Sand at base)	Quadra Sand	Coquitlam Drift Quadra Sand	Coquitlam Drift Quadra Sand
25			25					
MIS 3	(mid)	Olympia non glacial		Olympia sediments	Cowichan Head Formation	Cowichan Head Formation	Cowichan Head Formation	Cowichan Head Formation
57	Wisconsinan (early)	Semiahmoo/ Dashwood Glaciation	50					
MIS 4					Possession Drift	Dashwood Drift	Semiahmoo Drift	Semiahmoo Drift
71								
MIS 5	Sangamonian	Whidbey Interglaciation (MIS 5 or older)		Whidbey Formation	Muir Point Formation	Highbury sediments		
130								
MIS 6	Illinoian	unnamed glaciation MIS 6 or older		Double Bluff Drift	unnamed drift below Muir Point Formation		West Lynn Drift	Possible pre- Semiahmoo Drift (this paper)

1. Correlations of units predating the ca. 50 ka limit of ¹⁴C dating are tentative.
2. Point Grey peninsula and south Vancouver

Figure 2. Regional stratigraphy and geologic events in the Salish Sea/Georgia Depression region. The blue-tinted column pertains to the Greater Vancouver area, including Evergreen fjord. Sources: Armstrong, 1975; Clague, 1977; Armstrong and Hicock, 1979; Hicock and Armstrong, 1981; Alley and Hicock, 1986; Easterbrook, 1994; Hicock and Lian, 1995, 1999; Lian et al., 1995; Clague et al., 2005; Porter, 2011; Hebda et al., 2016.

elevated formerly depressed areas as much as 200 m asl (Clague and James, 2002). Rapid rebound, exceeding the rate of rising eustatic sea level during the waning stages of glaciations, resulted in the development of erosional surfaces. Lithostratigraphic units (summarized in Fig. 2; correlative geologic event units compared with the MIS record [Lisiecki and Raymo, 2005]) cannot necessarily be recognized or correlated without radiocarbon (¹⁴C) or other absolute dating methods. Nor can they be confidently assigned by counting backward from the most recent glacial sediments in exposures and drill cores; Quaternary sediments in the Fraser Lowland can be complicated palimpsests of sediments from multiple glaciations (Armstrong and Hicock, 1975, 1976). Erosion between deposition of units and fortuitous preservation at different elevations may complicate correlation of successions at any given location. Furthermore, units can be repeated as glaciotectonic allochthons (this paper). Correlation of units beyond the range of ¹⁴C dating is largely based on local stratigraphic context with ¹⁴C-dated units.

With two exceptions, ¹⁴C ages cited in this paper (Table 1) have been converted to mean calibrated years BP (cal yr BP) using the IntCal20 calibration curve (Reimer et al., 2020). Mean

calibrated values with a standard error between 50 and 1000 yr or >1000 yr were rounded to the nearest 10 or 100 yr respectively (Stuiver and Polach, 1977). The exceptions are nonfinite ages and finite ages whose error values extend beyond the limit of the calibration curve. In those cases, ¹⁴C years BP are reported. Because much of the work in the Fraser Lowland area preceded calibration to calendar years as a standard practice, significant ¹⁴C ages and ¹⁴C age ranges reported in previous work are shown in brackets as a convenience for the reader who might consult previous studies.

The structurally controlled low-lying areas including the Fraser Lowland and Salish Sea are called the Georgia Depression (Fig. 1). The stratigraphic framework of the Fraser Lowland was integrated into the regional stratigraphy by Armstrong et al. (1965; Fig. 2) for lands surrounding, and islands within, Puget Sound and Strait of Georgia regions of Washington State and British Columbia (now collectively referred to as the “Salish Sea” by geographic naming authorities in Canada and the United States) (Fig. 1). Because the inception, growth, and decay of the MIS 2 Cordilleran Ice Sheet are relatively well dated and documented, the MIS 2 ice sheet has been used to infer the behavior of pre-MIS 2 ice sheets in this region.

Table 1. Radiocarbon ages cited in this paper.

Lab no. ^a	Sample	Depth/ elevation (m)	Material	Fraction		D ¹⁴ C		¹⁴ C age		Calibrated age		Prob (%)	Mean (yr)	Error ^b (yr)	
				modern	±	(‰)	±	(BP)	±	(yr)	min.				max.
Core BH15-02: UTM N 5457368.8 E 508710.0, zone 10, WGS 84, surface elevation 129 m															
U184568	JJO230916-02	25.5/103.5	Detrital wood	0.1017	0.0008	898.3	0.8	18,360	60	22,168	22,431	95	22,300	130	
Core BH14-03: UTM N 5458047 E 509136, zone 10, WGS 84, surface elevation 91 m															
U184570	JJO241116-02	26.6/ 66.4	Twigs	0.0996	0.0008	900.4	0.8	18,530	70	22,299	22,595	95	22,450	150	
U184564	JJO230816-01	33.1/ 59.9	Plant fragments	0.003	0.0008	-997	0.8	46,700	2100	46,552	52,953	82.5	49,800	3200	
										53,179	55,000*	12.5	53,180	910	
U197772	JJO190517-01	46.3/ 46.6	Twig with bark	0.0311	0.0007	968.9	0.7	27,880	200	31,270	32,258	90.3	31,760	490	
										32,555	32,805	4.7	32,680	130	
U184563	BCW180816-M2	46.4/ 46.3	Plant fragments	0.0159	0.0008	-997	0.8	33,250	390	36,972	39,191	95	38,100	1100	
Core BH14-04: UTM N 5457952 E 509136, zone 10, WGS 84, surface elevation 93 m															
U184565	JJO 230816-02	40.4/ 64.6	Plant fragments in organic mud	0.0119	0.0008	988.1	0.8	35,630	520	39,768	41,642	95	40,700	940	
U184566	JJO 230816-03	41.9/ 63.3	Plant fragments	0.0122	0.0008	987.8	0.8	35,420	510	39,599	41,393	95	40,500	900	
U184567	JJO 061016-06	42.2/ 62.8	Plant fragments	0.0039	0.0008	996.1	0.8	44,600	1600	44,692	51,593	95	48,100	3400	
U184569	JJO 081016-01	46.5/ 58.5	Wood fragments	0.0003	0.0008	999.7	0.8	>50,300		*					
Core BH06-4: UTM N 54 UTM 5457291 E 508716, zone 10, WGS 84, elevation 127.08 m															
B221317 (d ¹³ C -27 ‰)	BH06-4	61/66.1	Wood	No data	No data			No data	18,350	90	22,110	22,445	95	22,280	170
Core BH06-6: UTM N 5457915 E 509030, zone 10, WGS 84, surface elevation 113.37 m															
U233898	JJO181019-01	57.6/ 55.8	Wood fragments	0.0018	0.0005	998.2	0.5	50,900	2400	*					
Core BH06-7: UTM N 5457984 E 509082, zone 10, WGS 84, surface elevation 102.9 m															
U233899	JJO 240818-03A	44.5/ 58.5	Plant fragments in organic mud	0.0432	0.0006	956.8	0.6	25,240	120	29,206	29,878	95	29,540	340	
U222938	JJO 240818-03B	44.5/ 58.5	As above	0.0537	0.0008	946.3	0.8	23,490	120	27,388	27,838	95	27,610	230	
U222939	JJO 220818-03	46.8/ 56.1	Plant fragments	0.0009	0.0005	999.1	0.5	>50300		*					
Core BH09-211 UTM N 5457852.08 E 509230.56 zone 10, WGS 84, Surface elevation 91.69 m															
U233900	JJO181019-02	44.5/ 47.0	Wood fragment	0.0375	0.0006	962.5	0.6	26390	130	30,316	30,986	95	30,650	340	
U197771	M16-3	46.8/47.2	Twig	0.0399	0.0007	960.1	0.7	25880	150	29,902	30,434	94.9	30,170	270	
										30,658	30,660	<0.1	30,660	1	
U197770	M16-2	46.8/47.2	Plant fragments	0.0327	0.0007	967.3	0.7	27470	190	31,150	31,746	95	31,450	300	
U197769	M16-1	46.8/47.2	Plant fragments	0.0221	0.0007	977.9	0.7	30620	280	34,475	35,520	95	35,000	520	
U215256	JJO240118-01	49/42.7	In situ root	0.0011	0.0005	998.9	0.5	54500	3700	*					

Core BH09-214 UTM N 5458321 E 509255 zone 10, WGS 84, surface elevation 85.76 m														
U215257	Box11-01	1954-08-26	Wood fragments	0.0952	0.0006	904.8	0.6	18890	50	22,593	22,979	95	22,790	190
U215258	Box12-01A	37.8/48	Wood fragments	0.0927	0.0006	907.3	0.6	19100	60	22,914	23,127	95	23,020	110
Port Moody Senior Secondary Ravine UTM N 5457752 E 0509536 zone 10, WGS 84, Elevation base of exposure ~68 m														
U170769	JJO230715-06	0/~71	Compressed detrital wood	0.0367	0.0005	963.3	0.5	26560	100	30,435	30,619	9.6	30,527	90
										30,696	31,089	85.3	30,890	200
Excavation for basement 567 Clarke Road, Coquitlam UTM ~5456625 N, 508036 E zone 10, WGS 84														
B524318 ($\delta^{13}\text{C} = -24.4 \text{ ‰}$)	J.J. Clague sample	~21/88	Plant fragments	No data	No data	No data	No data	18,160	50	21,990	22,259	95	22,120	130

²¹⁰Pu = UCIAMS W.M. Keck Carbon Cycle accelerator mass spectrometry laboratory at the University of California, Irvine, CA, USA; B = Beta Analytic Inc. 4985 S.W. 74th Court, Miami, FL 33155, USA.
¹⁴C An asterisk indicates the conventional radiocarbon age is too old to be converted into a calendar age.

Glacial and glaciomarine sediments deposited during MIS 4 (Semiahmoo glaciation), MIS 3 (Olympia interstadial; Hebda et al., 2016), and MIS 2 (Fraser glaciation) are correlated throughout the Salish Sea region (Fig. 2). Deposits along and on islands within the Salish Sea record single advances of ice sheets during both MIS 4 and 2. Incursion of the Cordilleran Ice Sheet was preceded by deposition of the time-transgressive (~33.5 to ~18.3 cal ka BP [~ 29 to ~ 15 ^{14}C ka BP]) pro-glacial Quadra Sand/Esperance Formation (Clague, 1976; Hicock and Lian, 1999; Clague et al., 2005).

However, within the Greater Vancouver area, a more complicated picture has emerged for MIS 2: local ice lobes interacted during the initial Coquitlam stage of the Fraser glaciation (equivalent to the Evans Creek stage in the mountains of western Washington State; Armstrong et al., 1965; Clark and Clague, 2020). Glacial lakes were initially ponded in mountain valleys north of the Burrard Inlet by damming of valley mouths by glacial ice in the Fraser Lowland (Lian and Hicock, 1993; Hicock and Lian, 1999; Hicock et al., 1999). Glaciers then descended the Capilano, Seymour, Lynn, Indian Arm, and Coquitlam drainages and interacted with ice in the Fraser Lowland. In the Capilano basin, the maximum age of the Coquitlam stage is limited by an age of $26,840 \pm 240$ cal yr BP ($22,600 \pm 240$ ^{14}C yr BP) (GSC 5705). An age of $25,840 \pm 100$ cal yr BP ($21,500 \pm 40$ ^{14}C yr BP) (GSC 2536) was obtained on detrital wood incorporated in Coquitlam stage drift, and an age of $26,040 \pm 130$ cal yr BP ($21,700 \pm 130$ ^{14}C yr BP) (GSC 2416) was obtained on detrital wood overlying Coquitlam drift in the Coquitlam River valley 8 km northeast of the Evergreen tunnel (Hicock and Armstrong, 1981; table 1 in Hicock and Lian, 1995; Fig. 1, AG).

A local retreat of glaciers followed the Coquitlam stage and has been termed the “Port Moody interstade” (Hicock and Armstrong, 1985; Fig. 2). Nonglacial sediments of the Sisters Creek Formation (Hicock and Lian, 1995) were deposited during this interval. They contain abundant in situ organic material. ^{14}C dating delimits this interstade to between ca. 22.4 to 21.2 cal ka BP (18.5–17.6 ^{14}C ka BP) (table 1 in Hicock and Lian, 1995). This age range also constrains the minimum age of the end of the Coquitlam stage. Paleoenvironmental indicators in Port Moody interstade sediments have been extensively studied (Hicock et al., 1982; Miller et al., 1985). The most comprehensive study by Lian et al. (2001) reevaluated previous interpretations of a cold, dry, glacial climate for the Port Moody interstade. They found that temperate, moist subalpine conditions existed near sea level during summer, alternating with drier conditions during winter. This interpretation envisions incursion of summer precipitation from the Pacific Ocean along the south margin of the Cordilleran Ice Sheet and displacement of winter storms farther south (Hicock et al., 1999) during long cold winters creating dry conditions.

The Port Moody interstade was succeeded by the climactic MIS 2 Vashon stage (Fig. 2), the maximum of late Pleistocene glaciation in this region. The Cordilleran Ice Sheet reached a terminus at the south end of Puget Sound after ~18.3 cal ka (~15 ^{14}C ka BP; fig. 8 in Easterbrook, 1992). ^{14}C ages on sea lion bone collected on Bowen Island at the mouth of Howe Sound immediately north of Vancouver, BC, indicate that the area was ice free before ~14.4 to 14.0 cal yr BP (13 to 12.5 ^{14}C ka BP) (Jackson et al., 2009). The area was inundated by the ocean with the rapid retreat of the ice sheet along a glacio-isostatically depressed calving margin at the termination of the Vashon stage. Glaciomarine sediments and deltas graded to high relative sea level, known as the

Capilano Sediments, were deposited on the glacio-isostatically depressed Fraser Lowland (Armstrong *et al.*, 1965; Armstrong, 1981).

Organic sediments deposited during the MIS 3 Olympic interstadial have been extensively ^{14}C dated. Paleoenvironmental indicators in these sediments have been investigated in detail (Heusser, 1977; Clague and MacDonald, 1989; Mathewes, 1991; Hebda *et al.*, 2016). Inferred climate during this interstadial ranged from similar to that of today to colder than present.

Glacial ice during the MIS 4 glaciation (Semiahmoo glaciation; Hicock and Armstrong, 1983; Fig. 2) had an extent comparable to MIS 2 in the Salish Sea region (Cosma *et al.*, 2008). Sediments associated with glaciations preceding the Semiahmoo glaciation have been found in the Greater Vancouver area (Fig. 2), but they are undated.

Rapid isostatic response of the crust to glacial loading and unloading in the Salish Sea region has been well documented by ^{14}C dating of relative sea-level indicators, including tilting of marine limits over short (tens of kilometers) distances, during and following rapid retreat of the Cordilleran Ice Sheet in the waning stages of the Fraser glaciation (Clague, 1983). Modeling of this isostatic response (James *et al.*, 2000; Clague and James, 2002) indicates that rapid isostatic rebound was due to low-viscosity (18.5×10^{18} Pa/s) in the asthenosphere and a thin (35 km) crust. Low mantle viscosity is driven by the underlying Cascadia subduction zone.

Materials and methods

Stratigraphic test borings (Fig. 3) were completed using sonic drilling methods under the direction of Golder Associates between 2000 and 2009 and SNC Lavilan, the tunnel contractor, between 2013 and 2015, following identical procedures. These borings yielded continuous, high-quality, 10.16-cm-diameter (4-in-diameter) cores. The deepest cores were obtained from the north half of the tunnel route where the tunnel depth is up to 50 m below the surface (the tunnel descends 90 m over 2.2 km from south to north). In core BH06-6, one of the deepest, core diameter was reduced to 6.4 cm (2.5 in) over the lowest 29 m. The cores were divided into 1.5-m-long (5-ft-long) sections, and two successive sections were placed in wooden core boxes (four sections for 6.4-cm cores) where they were photographed and

sampled for texture and other geotechnical properties by Golder Associates and SNC Lavilan. Each core was wrapped and sealed in heavy polyethylene sheeting for storage.

During our study, Golder Associates and SNC Lavilan drilling logs and photographs of cores were used to select cores that intersected sequences of apparent multiple glaciogenic diamictons and nonglacial sediments. In total, seven cores were chosen for detailed study. These were augmented by logs and photographs of nearby cores (Fig. 3). We used the textural data from Golder Associates and SNC Lavilan reports. Because the cores were collected for geotechnical purposes, texture was reported as gravel, sand, and fines (silt and clay) by Golder Associates and SNC Lavilan.

Cores were generally intact with greater than 80% recovery. Some were locally fragmented during previous description and sampling by Golder Associates. The deepest units typically were the most complete. Intervals up to 20 cm long had been removed locally from cores for textural analysis and other tests by Golder Associates and SNC Lavilan before our analysis. For these intervals, we relied on the results of textural analysis reported on the contractors' logs and photographs to fill in those blanks.

Our descriptions involved careful scraping of the core to remove exterior drilling detritus that obscured details. The exposed cores were photographed in 1.5-m lengths, and significant sedimentary structures and other features of interest were photographed down to centimeter resolution before sampling.

Nearby informative natural and artificial exposures

In addition to the cores, natural and artificial exposures, correlative to successions in cores (based on ^{14}C dating), were examined to enhance our interpretations (see "Stratigraphy and Sedimentology").

Stratigraphy and sedimentology

Core logging employed textural-based lithofacies codes (cf. fig. 10.1 in Benn and Evans, 1996) and incorporated the following sedimentary features:

- *Indicators of glaciotectonic deformation.* These included penetrative shear planes with slickensides, breccia, plucked organic intraclasts, and evidence of ductile deformation (Figs. 4, 5,

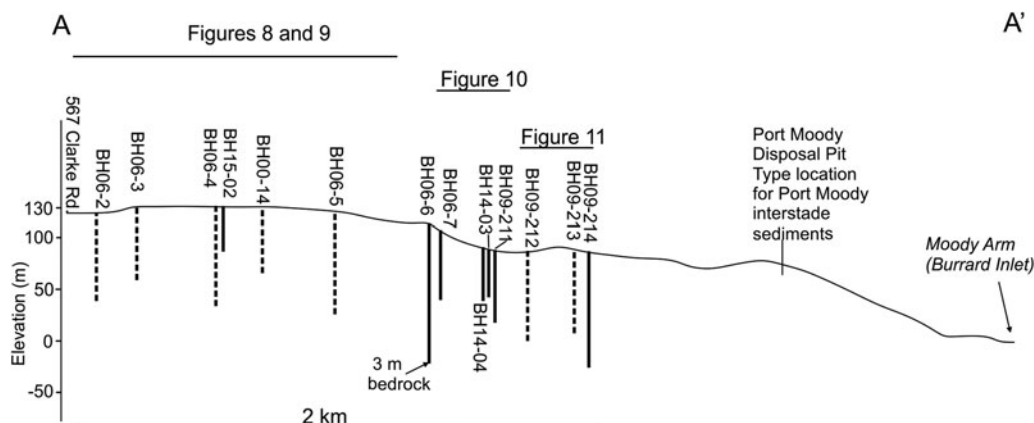


Figure 3. A 3.5-km-long topographic profile of the Evergreen tunnel showing locations of borehole logs and a basement excavation examined in this study (A-A' in Fig. 1C). Dashed lines are cores logged by Golder Associates but not physically examined during this study. The Port Moody Disposal Pit is projected on to the profile.

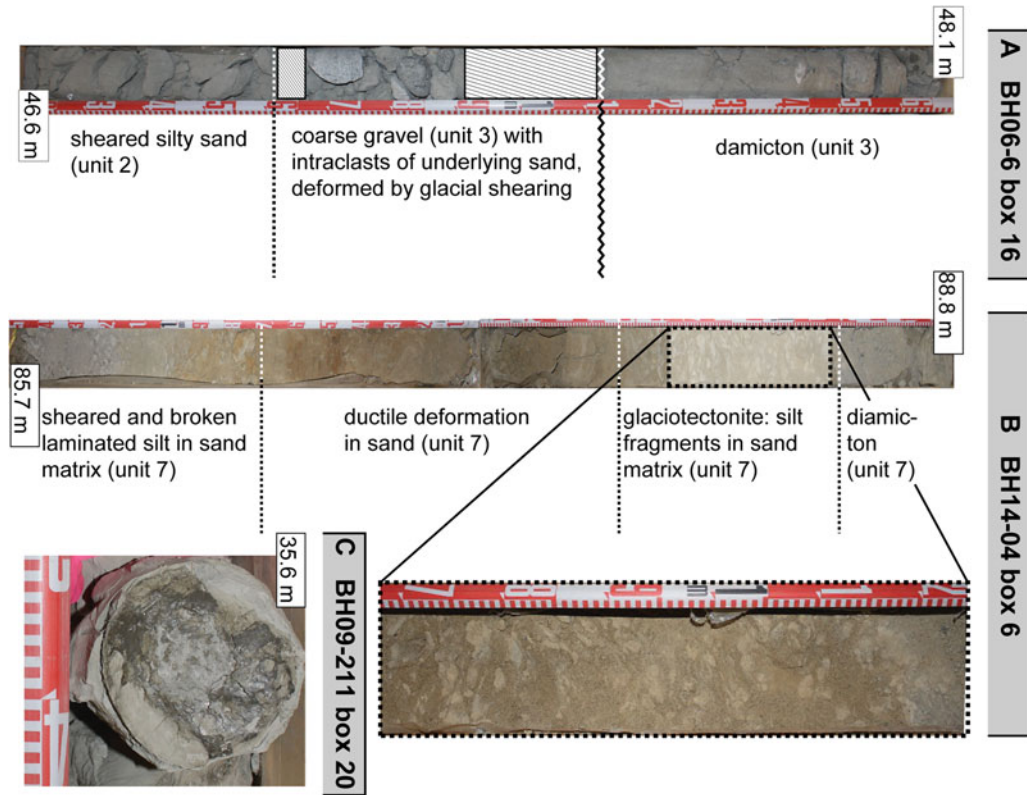


Figure 4. Examples of unconformity and shear features. Numbers are elevations; patterned boxes are sampled intervals. (A) Gravel overlying diamicton of unit 5; sheared silty sand lies below an eroded surface. Gravel and underlying sand were deformed by glacial overriding during MIS 4. (B) Composite photograph of a brecciated zone created by overriding of the Cordilleran Ice Sheet during the deposition of unit 7. (C) View from top of slickensides in intensely sheared clayey silt.



Figure 5. Exposure directly below the ground surface in the Allard gravel pit, Coquitlam (Fig. 1 (elevation ~188 m asl)), showing formerly stratified pebbly sand and silty sand deformed by overriding by glacial ice during deposition of unit 7 diamicton. It is an analog for glacioteconites intersected by drilling (e.g., Fig. 4B). The contact between unit 7 and underlying glacioteconized sediments is gradational (dotted lines define prominent deformed beds in intact blocks within the glacioteconite). Plucked peat and wood have been incorporated in this glacioteconized zone.

and 6C). In cases where indicators of glaciotectionism were found, we assumed that they were products of glacial overriding, regardless of the presence or absence of till overlying them. Where absent, till was assumed to have been removed by post-glacial or interstadial erosion.

- *Erosional unconformities.* These show a distinct sand or sand and gravel lag on an erosional surface. The lag commonly contains intraclasts derived from the underlying unit. Contacts lacking these features were assumed to be conformable or disconformable. In some cases, unconformities were deformed by subsequent glacial overriding (Fig. 4A).
- *Buried soils.* These were recognized from oxidation of sediment below an unconformity. Pedogenesis indicates intervals of sub-aerial exposure (Fig. 6A, Table 2).
- *Organic units.* These include peat and organic-rich mud (Fig. 7B and C). They mark intervals of ice-free conditions. All were sampled for ^{14}C dating and future paleoenvironmental study. Some units were determined to be allochthonous, that is, they were subsequently displaced by glaciotectionism.
- *Bioturbation.* This includes burrows in subaerial peaty organic units (Fig. 7A and B) and in fine sand, silt, and clay units in subaqueous sediments. The latter, in the absence of dropstones, were interpreted as indicating glaciomarine or glaciolacustrine conditions.
- *Primary bedding and soft-sediment deformation.* Laminated or rhythmically laminated fine sand and silt, together with a lack of dropstones, were interpreted as reflecting distal glaciomarine or glaciolacustrine conditions. Slump structures and dewatering structures were interpreted as indicators of rapid sedimentation.
- *Dropstones.* An increase or decrease in the frequency of dropstones in a core was interpreted as indicating increasing or decreasing proximity to glacial ice, respectively, in glaciomarine or glaciolacustrine environments (Fig. 7C).

Because cores were described at centimeter scale in sequences up to 100 m long, lithofacies codes were generalized into stratigraphic columns for presentation (Figs. 8–11) under the headings of diamicton, gravel, sand and silt, and clay along with symbols denoting glaciotectionic and sedimentological features to enhance recognition of glacial and nonglacial events. Eight units bounded by unconformities or major changes in sedimentation were identified. Table 3 presents examples of how we converted facies codes into the lithostratigraphic logs shown in Figures 8–11.

Intervals containing organic sediments were sampled for ^{14}C dating (Table 1). The samples were sent to the W.M. Keck Carbon Cycle accelerator mass spectrometry laboratory at the University of California, Irvine, CA, USA. Remanent magnetic polarity was determined for select samples at the Paleomagnetism Laboratory of Pacific Geoscience Centre, Sidney, BC. Fragments of obsidian were found as distinct bands in one core. Samples of the obsidian were submitted to R. Reimer, Department of Archaeology, Simon Fraser University, for X-ray fluorescence analysis to match them with known obsidian occurrences.

Figures 8 to 11 present the most informative sequences that allowed us to reconstruct glacial events in the area, including a deep basement excavation 400 m south of the south portal (Fig. 9). The depth of drilling for each borehole was determined by the depth of the proposed tunnel below the surface; drilling usually terminated 10 to 20 m below it. The surface elevation near the south end of the tunnel is highest; the terrain there is

nearly level and the tunnel depth is shallow (Figs. 3 and 8). Consequently, Figures 8 and 9 are the most informative for interpreting sediments deposited during MIS 2. The longest records were found in cores at midtunnel position (Fig. 10). Borings coincide with the steepest grades of the northward descending hill (Fig. 3). MIS 2 glacial sediments have been eroded in part from the sequence. Pre-MIS 4, MIS 4, and MIS 3 sediments are present in cores from this area. Some have glaciotectionic allochthons. However, cores that intersect sequences most affected by glaciotectionism are located at the north end of the tunnel (Fig. 11). We discuss the stratigraphy and glaciotectionism recorded in the tunnel cores in the following sections, from the oldest to youngest sediments.

Units 1 and 2

Units 1 and 2 were only fully intersected by drilling in BH06-6 (Fig. 10), which is the only boring to reach bedrock. Unit 1 consists of 2 m of silty gravelly diamicton containing Coast Mountains provenance clasts. It was deposited on conglomerate of the Eocene Huntingdon Group and is overlain gradationally by unit 2, which, above its lower 4 m, comprises 58 m of sporadically bioturbated, laminated to thinly bedded silt and fine sandy silt. Unit 2 is the thickest unit in Evergreen fjord, extending from about 19 m below mean sea level to about 43 m above it. The 4-m-thick gradational contact between units 1 and 2 is marked by a fining-upward sequence of silt and fine sand beds containing pebble and cobble-size dropstones (Fig. 7B and D). Many beds in unit 2 display soft-sediment deformation features such as diapirs and dewatering structures. The uppermost 2 m of unit 2 coarsens to fine sand that is abruptly truncated along an erosional contact by gravel. The sand, erosional contact, and overlying gravel have been sheared. Samples at 7 and 13 m below sea level in unit 2 were determined to be magnetically normal (Enkin, R., written communication, 2019) indicating that it was probably deposited during the Brunhes magnetic chron, which spans the past 780,000 yr. Because the cores were unoriented, no other paleomagnetic information could be gleaned from them beyond polarity. Unit 2 was only intersected as an autochthonous unit in BH06-6, BH06-7, and BH09-211. It is incorporated in allochthons in borings in the area at the north end of the tunnel (Fig. 11). Consequently, it is likely extensive within the Evergreen fjord fill.

Unit 3

Unit 3 consists of matrix-supported, indurated diamicton containing striated Coast Mountains provenance clasts and interstratified sand and gravelly sand. This unit was intersected in boreholes BH06-6, BH14-4, BH06-7, and BH09-211 (Fig. 10). Cores BH06-6, BH06-7, and BH09-211 contain the most complete records and are free of allochthonous units, unlike BH14-3, where inversion of ^{14}C ages indicates glaciotectionic repetition of units (Fig. 10). In BH09-211, unit 3 occurs between 27.6 and 40.7 m asl. The lower contact of unit 3 is an unconformity truncating unit 2. Sand, gravelly sand, and gravel less than 1 m thick overlie the unconformity. The unconformity and the upper few meters of unit 2 are pervasively sheared. In BH06-7 and BH09-211, the diamicton is succeeded by a fining-upward sequence of sediments, the lower part of which contains dropstones. In cores BH06-7 and BH09-211, an upper diamicton overlies the fining-upward sequence and the fining-upward sequence

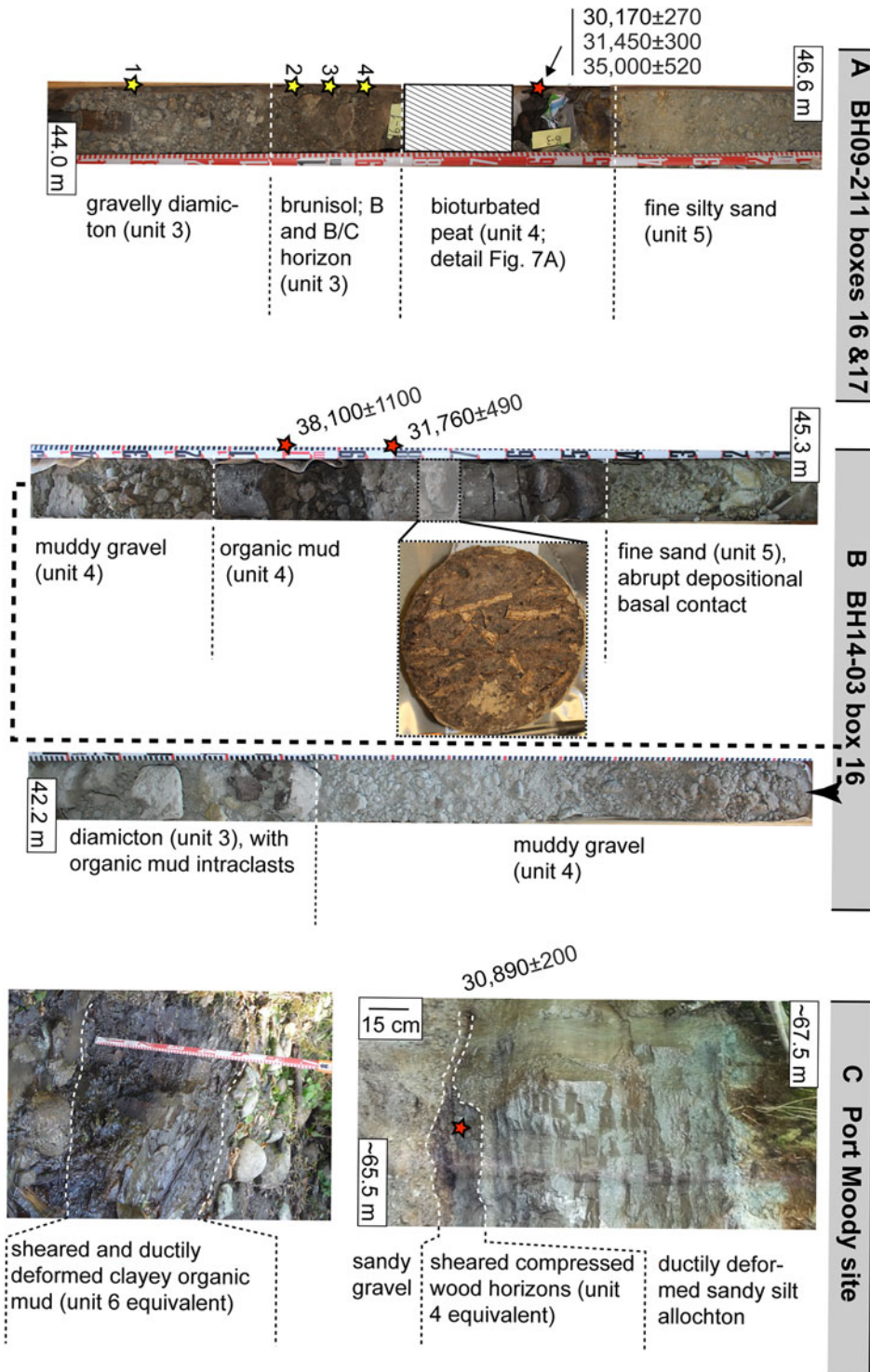


Figure 6. Buried soil and organic sediments of unit 4 and adjacent sediments. (A) Soil B and B/C horizons developed in unit 3 diamicton in BH09-211 (yellow stars show the locations of chemical sample for analysis; Table 2). (B) Overconsolidated organic mud rich in plant fragments of unit 4. This mud conformably overlies muddy gravel and diamicton of unit 3. The organic sequence is abruptly overlain by silty fine sand of unit 5. (C) A 3-m-thick exposure of sheared and ductily deformed woody, organic-rich mud in a ravine near Port Moody Senior Secondary School. These sediments are analogs for glaciotectionized unit 4 sediments intersected in cores. Patterned areas are intervals sampled or fragmented during prior logging by Golder Associates.

Table 2. Analysis of paleosol in BH09-211 (Figs. 6A and 10).^a

Sample (JJO)	Depth (m)	Munsell color	Soil horizon ^b	Extraction method/analysis					
				Sodium pyrophosphate/ ICP-OES ^c		Ammonium oxalate/ ICP-OES		Combustion	
				Al %	Fe %	Al %	Fe %	N %	C %
JJO250419-05	47.36	7.5YR 4/2 to 10YR 4/2	Bm, Bfj	0.093	0.037	0.29	0.061	< 0.05	0.76
JJO250419-04	47.41	10YR 5/1	Bm, Bfj	0.081	0.032	0.24	0.055	< 0.05	0.66
JJO250419-03	47.51	5YR 7/1	B/C	0.057	0.029	0.12	0.05	< 0.05	0.35
JJO250419-02	47.71	5YR 7/1	C	0.041	0.02	0.08	0.046	< 0.05	0.091

^aAnalysis by British Columbia Ministry of Environment, Knowledge Management Branch, Analytical Chemistry Section.

^bHorizon interpretation based on criteria of Agriculture and Agri-foods Canada (1998).

^cInductively coupled plasma optical emission spectroscopy.

is sheared. In BH09-211, the two diamictons are separated by 10 m of gravelly sand fining upward into fine stoneless sand and silt.

Unit 4

Unit 4 consists of thin (5–30 cm) beds of highly compressed, locally bioturbated organic deposits and sandy and gravelly sediments that contain disseminated detrital organic material (Fig. 6). A truncated paleosol is present in the upper 20 cm in the

uppermost diamicton of unit 3, unconformably overlain by the organic deposits of unit 4 in BH09-211. The organic deposits yielded ages of $30,650 \pm 340$ cal yr BP (U233900), $30,170 \pm 270$ cal yr BP (U197771), $31,450 \pm 300$ cal yr BP (U197770), and $35,000 \pm 520$ (U197769) cal yr BP (Fig. 10, Table 1). These ages place an upper age limit on the underlying paleosol and diamicton. An unsheared, in situ root is present in the sheared sediment underlying the upper diamicton of unit 3. Assuming that this root was related to a forest under which the Brunisolic paleosol developed, its age of $54,000 \pm 3700$ ¹⁴C yr BP (U215256) places a

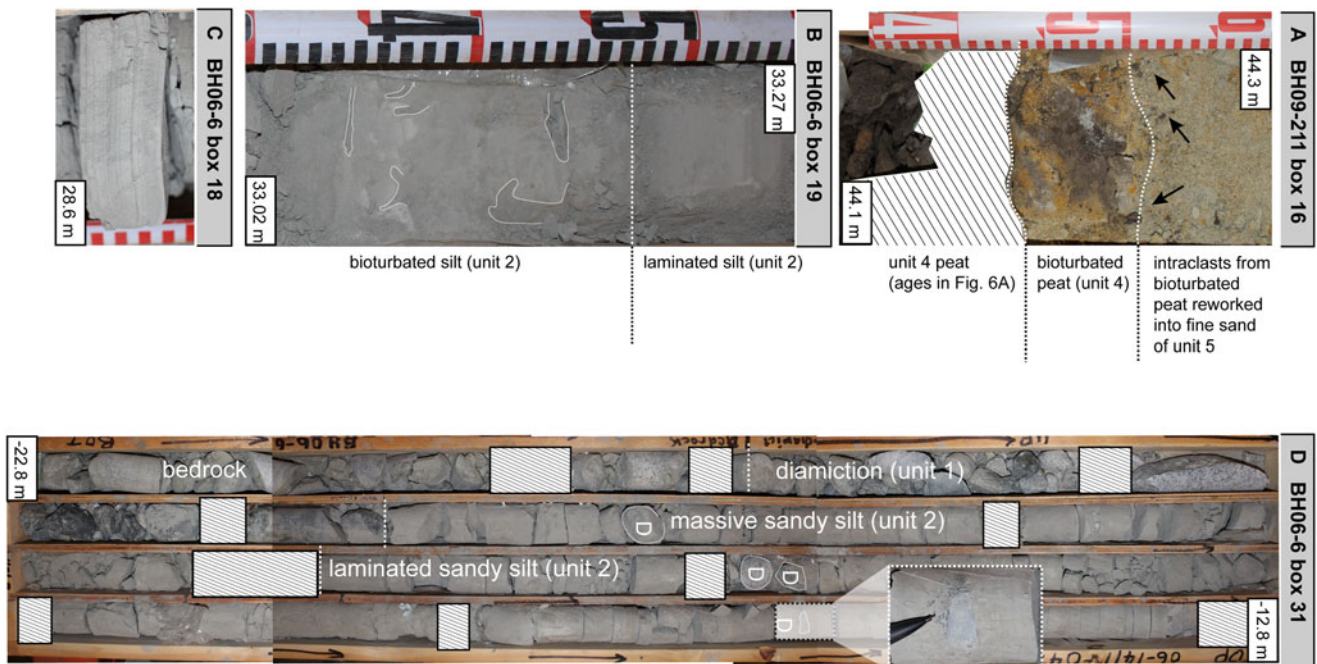


Figure 7. Examples of bioturbation and other sedimentary structures. (A) Detailed view of unit 4 peat in Fig. 6A. Peat is extensively bioturbated (trace fossils *Naktodemasis boweni* or *Taenidium boweni*; MacEachern, J., personal communication, 2019). Peat is abruptly overlain by fine sand containing intraclasts of peat. (B) Laminated silt overlying bioturbated laminated silt (ichnogenus *Planolites*; J. MacEachern, J., personal communication, 2019). (C) Graded rhythmites in unit 2. (D) Basal 10 m of BH06-6, the only boring to reach bedrock beneath sediments infilling Evergreen fjord. The basal diamicton is unit 1. Sediments are Marine Isotope Stage (MIS) 4 or older and show a typical fining-upward sequence that is repeated in overlying glacial sequences, from diamicton to sand and sandy silt with dropstones. Detail shows the uppermost dropstone. The overlying 60 m (unit 2) is free of dropstones, with the exception of rare dropstones in the upper 5 m.

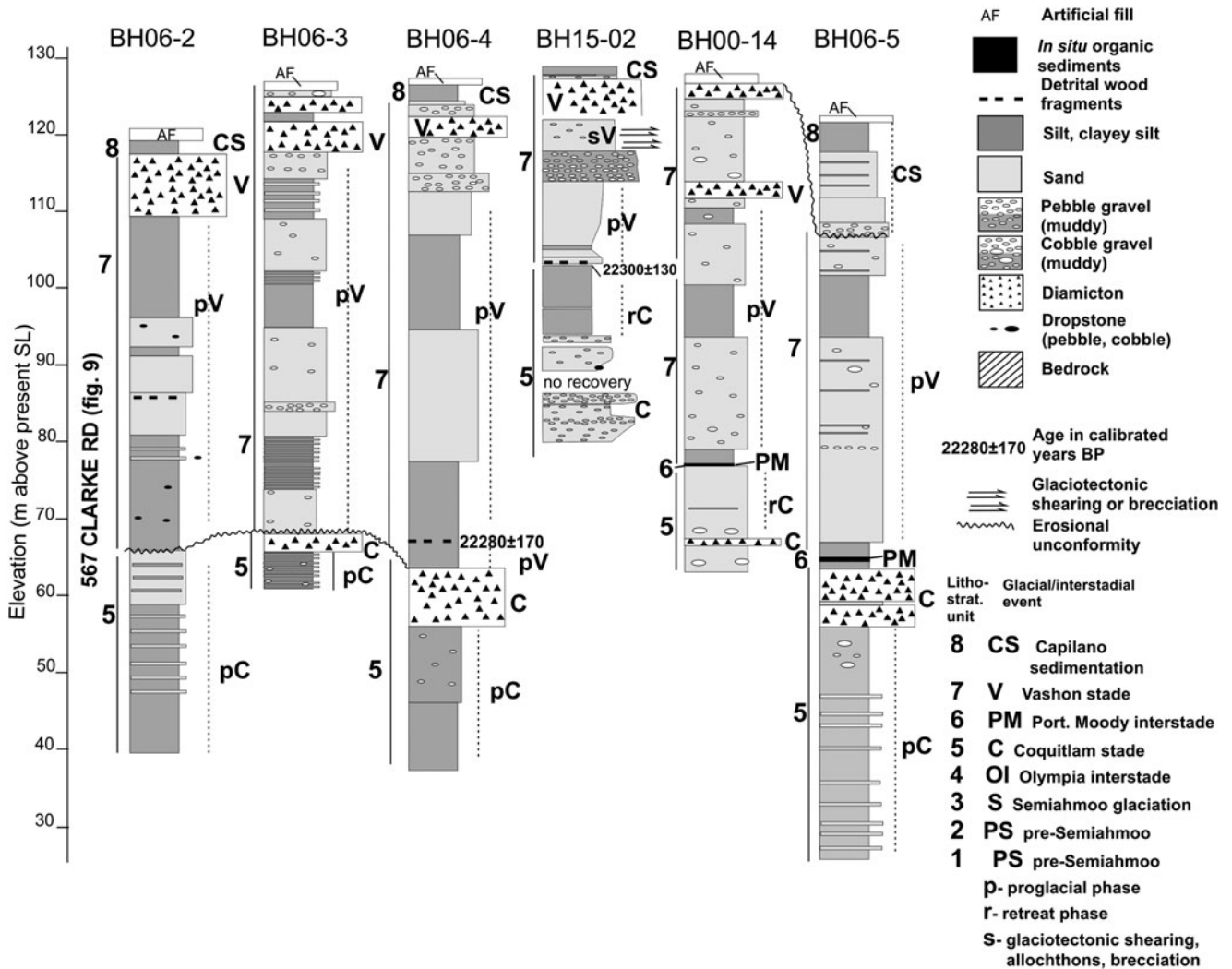


Figure 8. Logs of cores along the southern portion of the Evergreen tunnel (Fig. 3). BH15-02 was physically studied and was used as a reference for stratigraphic interpretation of Golder Associate logs shown in this figure. These logs include sediments of units 5 to 8. Glaciotectionic deformation is extensive below unit 7 diamicton in BH15-02 and resembles the deformation in the gravel pit exposure shown in Fig. 5.

maximum age on the paleosol and unit 4 (note: the age lies beyond the IntCal20 calibration curve).

Unit 5

Unit 5 unconformably overlies Unit 4 and is composed of mud, sand, gravel, and diamicton. It also includes sheared and allochthonous sediments (Figs. 8, 10, and 11). Fragments of obsidian found in distinct bands within the lowest diamicton in BH09-214 (Fig. 11) have a provenance in the Mt. Garibaldi volcanic area, 60 km to the north (Reimer, R., written communication, 2023).

Unit 5 is most complete in core BH09-211. Starting about 44 m asl, stoneless sand abruptly overlies unit 4 peat. The lowest 10 cm of the sand contains intraclasts of peat (Figs. 6A and 7A). The sand coarsens upward into gravelly sand, which is in turn overlain by interbedded diamicton and gravel. The diamicton contains striated Coast Mountains provenance stones and is overlain by gravelly sand to silt. The latter deposits can only be distinguished from similar overlying unit 7 sediments, where they are overlain by peat or in situ woody material of unit 6 (e.g., Fig. 8, BH06-5) or where unit 5 sediments are separated from overlying

unit 7 sediments by an erosional unconformity (Fig. 8, BH00-14; Fig. 10, BH06-6, BH14-04, and BH09-211).

Examples of allochthonous unit 4 sediments incorporated into unit 5 are present in BH14-03 and BH14-04 and in a natural exposure between these boreholes near the north portal of the tunnel (Fig. 1C, PMS). There, beds of detrital wood and clayey silt dated to $30,530 \pm 90$ cal yr BP (U170765; Fig. 6C) have been sheared by subsequent glaciotectionism.

Unit 6

Unit 6 consists of in situ organic-rich beds ranging from 10 to 50 cm in thickness that occur sporadically in the cores. Their lowest occurrences are 60–65 m asl, resting on unit 5 deposits. The best examples can be found in cores BH00-14 and BH06-5 (Fig. 8), the Clarke Road basement excavation (Fig. 9), and core BH14-03 (Fig. 10). Plant fragments at the Clarke Road site have been dated to $22,130 \pm 140$ cal yr BP (B524318). Plant fragments in an in situ unit 6 bed in BH14-03 (Fig. 10) yielded a similar age of $22,450 \pm 150$ cal yr BP [U184570]; Fig. 8, Table 1). In cores lacking unit 6, a prominent unconformity above 65 m asl

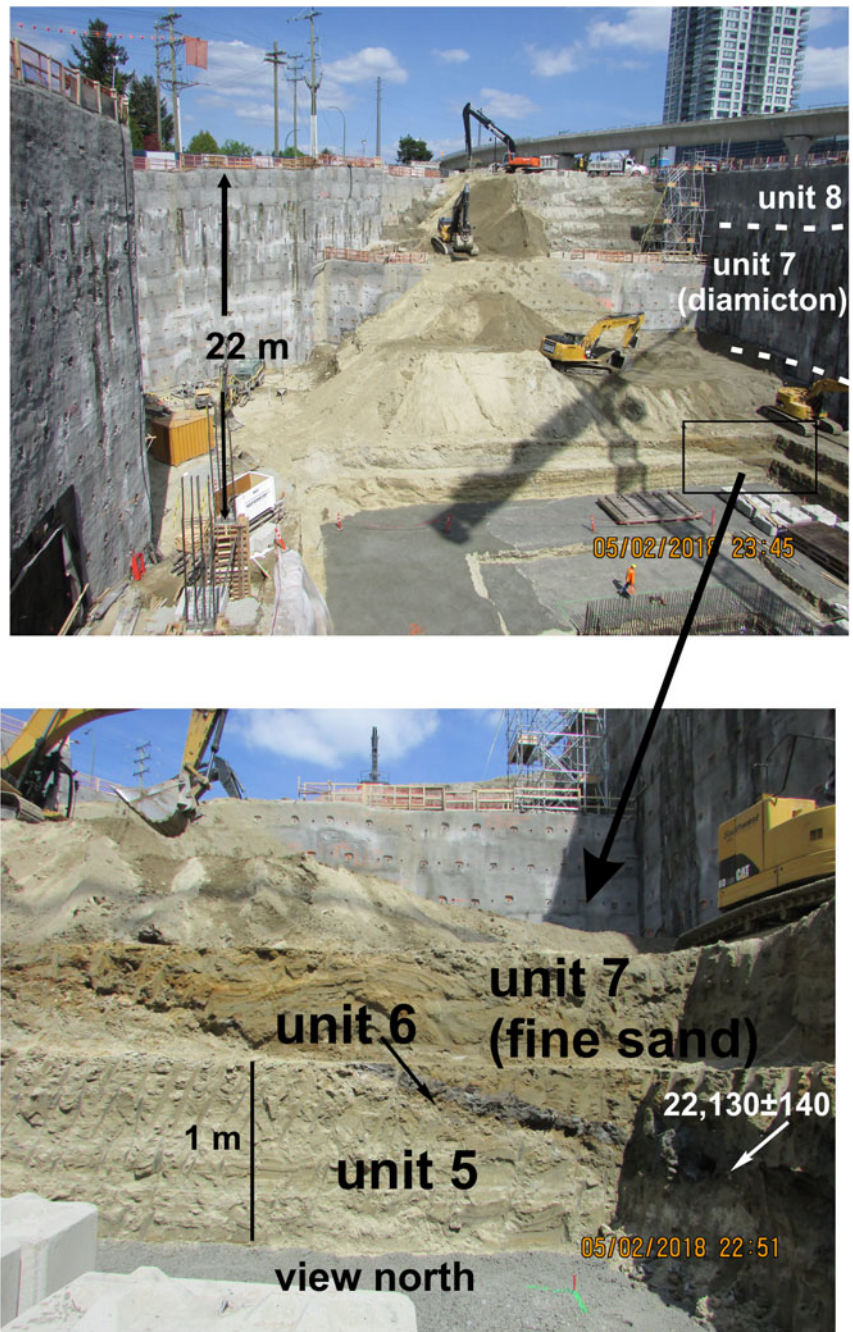


Figure 9. Apartment tower basement excavation at 567 Clarke Road, 400 m south of the south tunnel portal. Top, Unit 7 diamiction and gravel are overlain by unit 8. Stratigraphy was projected onto the shotcrete-covered wall from a light rail transit guideway boring (Golder Associates, 2010; core BH09-201). Bottom, The calibrated age of the peat bed constrains it to unit 6.

separates units 5 and 7 (e.g., Fig. 8, BH06-02 and BH06-03; Fig. 10, BH06-6).

Unit 7

Unit 7 is a coarsening-upward sequence beginning with stoneless silt and grading into coarse sand, gravel, and diamiction containing striated clasts from the Coast Mountains (e.g., Fig. 8, BH00-14). It unconformably overlies unit 6 (Fig. 9) or an unconformity eroded into unit 5 (e.g., Fig. 8, BH06-3). The silty lower part of the unit contains detrital woody fragments yielding ages of $22,280 \pm 170$ cal yr BP (B221317), $22,300 \pm 130$ cal yr BP (U184568) (Fig. 8, BH06-04 and BH15-02), $22,280 \pm 170$ cal yr BP (U215257), and $22,300 \pm 130$ cal yr BP (U215258) (Fig. 11). The ages are within

the range of ages determined on material from in situ beds of unit 6. Consequently, the detrital material was eroded from unit 6. They limit the maximum age of unit 7. Unit 7 ranges from 20 to 55 m thick (all cores in Fig. 8). Like units 3 and 5, this unit terminates upward in diamiction that overlies up to 10 m of sheared sediments (Figs. 5 and 8, BH15-02).

Unit 8

Unit 8 overlies unit 7 diamiction or an unconformity truncating older sediments. It generally fines upward from stony sand to bioturbated sand and silt. It has a character and occupies a position analogous to the generally fining-upward sequences in units that overlie the diamictions in units 3 and 5. Sandy beds of unit 8 (<1 m thick) underlie

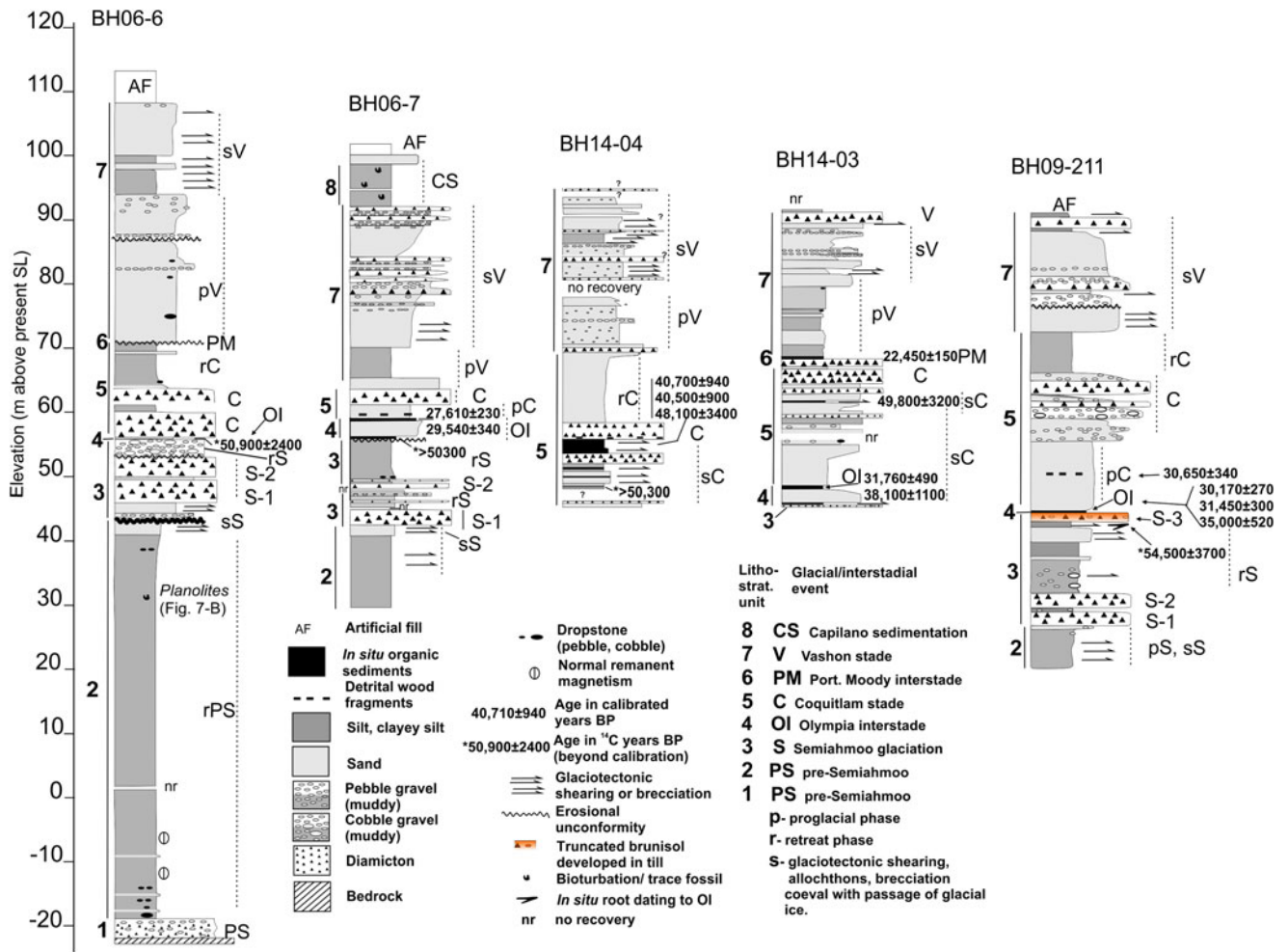


Figure 10. Logs of boreholes along the north-central portion of the Evergreen tunnel (Fig. 3).

the surface or artificial fill in all cores (Fig. 8). Unit 8 thickens in a northerly direction and with descending elevation (thicknesses of unit 8 are about 5 m in BH06-7 (Fig. 10) and up to 25 m at the north end of the tunnel (Fig. 11). Buried soils within unit 8 are found in BH09-212 and BH09-214 (Fig. 11).

Interpretation of stratigraphic units

Interpretation of the lithostratigraphy is presented in the following sections and generalized in a series of schematic diagrams in Figure 12. Table 4 summarizes how we created event codes used in Figures 8–11 to indicate events such as glacial advance, direct glacial sedimentation, glaciotectionism, glacial retreat, and subaerial erosional/soil-forming events, along with their correlation to the regional stratigraphic framework.

Units 1 and 2: Pre-Semiahmoo drift or drift from an early Semiahmoo glaciation

Unit 1 is interpreted to be till (PS) deposited when glacial ice from the Coast Mountains filled Evergreen fjord. The gradational fining-upward transition to unit 2 and the conformable contact of the two units reflect calving retreat of glacial ice following the deposition of the till. The 48 m of almost entirely stoneless silt overlying the gradational contact with unit 1 was likely deposited in a distal

glaciomarine or glaciolacustrine environment (rPS). Erosion of the uppermost sediments of unit 2 at 43 m asl (Fig. 10) indicates significant postdepositional isostatic rebound and subaerial exposure. Units 1 and 2 are undated but underlie sediments that are clearly MIS 4 in age (Figs. 2 and 10). The only age control on unit 2 is normal remanent magnetism indicating an age of <780,000 yr (Roberts and Turner, 2013). Two possibilities exist for the ages of units 1 and 2: deposition during MIS 6 (or an older glaciation) or deposition during an earlier part of MIS 4. Regardless of age, the sequence indicates that the area was isostatically depressed following retreat of an ice sheet from the area, then eroded after emergence.

Unit 3: Semiahmoo Drift of the Semiahmoo glaciation (MIS 4)

We assign unit 3 to Semiahmoo Drift (formalized by Hicock and Armstrong, 1983). Diamicton overlying the unconformity at the top of unit 2 (e.g., Fig. 10, BH09-211) is indurated and contains Coast Mountains provenance stones. These characteristics, and the glaciotectionic shearing of underlying sediments exerted by the overriding basal glacial ice indicates its genesis as till.

Collectively, sediments in unit 3 record a glacial cycle. pS represents proglacial sediments that were sheared (sS) beneath overriding basal ice that deposited tills S-1 and S-2. rS is a fining-upward sequence deposited during glacial retreat in a glaciomarine or glaciolacustrine environment. There is a third till

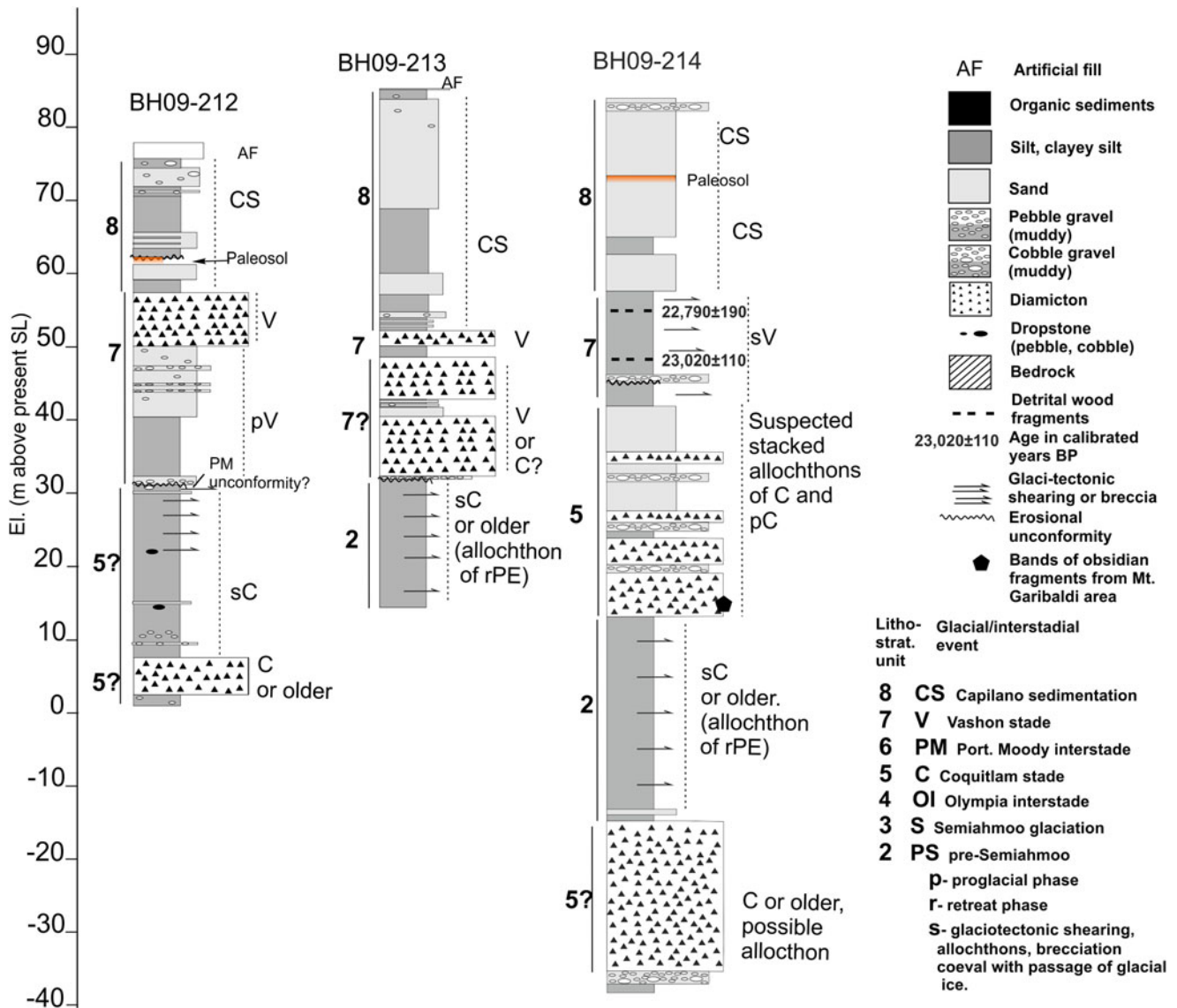


Figure 11. Logs of boreholes in the north portal area (Fig. 3).

(S-3) in BH06-7 and BH09-211. It is not clear based upon existing evidence whether S-1, S-2, and S-3 represent two or three glacial advances during MIS 4 or if the stack of tills and intervening sediments were emplaced during a single multiphased advance.

An age of $50,900 \pm 2400$ ^{14}C yr BP (U233898) was determined on subaerial organic material in a silt overlying S-1 and S-2 in BH06-6 and $>50,350$ ^{14}C yr BP (U222939) on subaerial organic material overlying S-1 and S-2 in BH06-7. These ages assign the deposition of underlying tills and related glaciectonism to MIS 4 (or older). An age on an in situ root below S-3 in BH09-211 is discussed in the next section.

Unit 4: Cowichan Head Formation and buried soil of the Olympia interstadial (MIS 3)

We assign unit 4 to the Cowichan Head Formation (formalized by Armstrong and Clague, 1977). It includes sediments accumulated in fens and bogs in poorly drained depressions on the surface of MIS 4

sediments. Detrital sedge, sphagnum, and wood are common within this unit (Fig. 6B). Investigations of the paleoenvironments recorded in sediments of similar ages around the Georgia Depression are referenced in the “Stratigraphic Framework” section. Conditions ranged from colder and drier to comparable to the present.

The truncated Brunisolic paleosol in BH09-211 is unique in the record of MIS 3 sediments in the Fraser Lowland. The sediments hosting the paleosol are oxidized, with increasing red-yellow hue upward. The overlying organic sediments were bioturbated under subaerial conditions by burrowing insects that left ichnofossils of the species *Naktodemasis boweni* or *Taenidium boweni* (MacEachern, J., personal communication, 2019).

Standard extraction analyses (Table 2) show a corresponding upward increase of Fe and Al indicative of pedogenic illuviation. Lack of clay enrichment makes Bfj the most appropriate designation for this horizon under the Canadian Soil Classification scheme (Agriculture and Agri-foods Canada, 1998). This assignment places the paleosol in the Brunisolic Great Group, typical of forest conditions that are common in the area today. Such soils require hundreds

Table 3. Examples of conversion of detailed facies codes to generalized lithostratigraphic logs from BH06-6 and BH09-211.

Unit	Description	Facies code ^a	As portrayed in Fig. 11	Comments
1	Clast-supported massive diamicton	Dcm	Alternating gravel and solid triangles	
1/2	Fining-up sequence of sandy silt with scattered fine sand beds, both with dropstones	Fm(d)Suf(d)	Sand with pebble and cobble dropstones; prominent sand beds shown	Transition zone included in unit 2
2	Massive to rhythmically laminated silt; local dewatering structures, bioturbation	Fm, Fl	Silt; prominent trace fossils	
3	Sheared muddy gravel	Gm(s)	Muddy gravel with glaciotectionic shearing symbol	
3	Massive sand		Sand shown as distinct unit	
3, 5,7	Stony massive diamicton	Dmm	Diamicton	
3	Bouldery, poorly sorted gravel	Gm	Pebble gravel, cobble gravel, or muddy equivalents	
4	Organic-rich mud	No facies code	Silt texture solid dark fill	
4 and 8	Paleosols developed in diamicton or sand	No facies code	Paleosol symbol	
5	Sand fining upward to massive silt with dropstones	Suf(d), Fm	Sand decreasing in coarseness upward to silt; dropstone symbols in unit	Interstratified coarse beds shown as distinct units
7	Glaciotectionically sheared sand	Sm(s)	Sand with shearing/brecciation symbol	

^aFrom table 10.1 in Benn and Evans (1996).

of years to more than a thousand years to form under a climate analogous to the present one in the Evergreen fjord area (Smith et al., 2011). Its formation and truncation document an episode of glacio-isostatic rebound that lifted the land above sea level followed by subaerial erosion before the deposition of overlying peat.

The age of $54,500 \pm 3700$ ¹⁴C yr BP (U215256) on the in situ root that grew in previously sheared sediment below S-3 in BH09-211 (Fig. 10) is near the practical limit of ¹⁴C dating. This age occurs at the base of a conformable sequence of sediments (no ¹⁴C age inversions). However, because of uncertainty as to the reliability of this as a finite age, the end of MIS 4 (ca. 60,000 cal yr BP; Lisiecki and Raymo, 2005; Siddall et al., 2008) is the surest lower age limit for unit 4 and the upper age limit for unit 3. The youngest limiting ages for unit 4 fall in the 33–29 cal ka range (Fig. 10, BH06-6, BH14-4, BH06-7, and BH09-211). The presence of organic sediments, a paleosol, and evidence of subaerial erosion, together with ¹⁴C ages on correlative sediments elsewhere in the greater Vancouver area, indicate ice-free conditions throughout MIS 4 in the Evergreen fjord area.

Unit 5: Coquitlam Drift of the Coquitlam stade (early MIS 2)

The MIS 2 Fraser glaciation in the North Vancouver and Port Moody-Coquitlam areas (Fig. 2) has long been subdivided into the Coquitlam stade, the Port Moody interstade, and the Vashon stade (Hicock and Armstrong, 1983, 1985). The Vashon stade was followed by an interval of high relative sea level during which Capilano sediments were laid down. In total, tens of meters of sediment were deposited in Evergreen fjord during MIS 2 (Figs. 3 and 8–11).

We assign unit 5 to the Coquitlam Drift (formalized by Hicock and Armstrong, 1981). Sedimentary designators pC, sC, C, and rC represent a glacial cycle starting with proglacial sediments (pC), deposited on unit 4 organics, then glacial ice cover (C), and finally deglaciation (rC). sC designates glaciotectionically sheared sediments formed during deposition of diamicton C (Fig. 10, BH14-04).

Unit 5 sediments are assigned to the Coquitlam stade based on ¹⁴C ages and stratigraphic position. Diamicton C is indurated, contains Coast Mountains provenance stones, and overlies sheared sediments of pC that were deformed by overriding basal ice. The diamicton is interpreted to be till deposited during the initial advance of the MIS 2 glaciers into the Evergreen tunnel area. Gravelly sand to silt was deposited during glacial retreat and inundation of the area (rC) following till deposition (C).

Obsidian fragments found in BH09-214 (Fig. 11) do not exist in situ in the Fraser Lowland. As previously noted, they were geochemically matched with known occurrences at the Mount Garibaldi volcanic center, 60 km to the northwest in the Coast Mountains (Fig. 1). It follows that glaciers advanced from that area during the Coquitlam stade. The most direct route is via the Pitt River watershed, which has its headwaters near Mount Garibaldi. The presence of obsidian fragments in distinct bands likely reflects passage of basal ice over obsidian outcrops rather than simple reworking from older drift units. This finding supports previously reported ice-flow indicators (Hicock and Lian, 1999) that indicate glacier ice flowed into the Evergreen fjord area from the Pitt River watershed during the Coquitlam stade (Fig. 1). Based on the presence of Coquitlam till throughout Evergreen fjord, we conclude that glacier ice at the maximum of the Coquitlam stade was sufficiently extensive to traverse the underlying Evergreen fjord fill and extend beyond the area.

Unit 6: Sisters Creek Formation of the Port Moody interstade (MIS 2)

We assign unit 6 to the Sisters Creek Formation (formalized by Hicock and Lian, 1995). Following retreat of glacial ice from the Evergreen fjord area and glacio-isostatic rebound, an open spruce–fir forest became established on recently deglaciated surfaces (Hicock et al., 1982; Miller et al., 1985; Lian et al., 2001). At the Port Moody Disposal Pit (a Sisters Creek parastratotype; Figs. 1 and 3), the boles of fallen trees from that forest are well

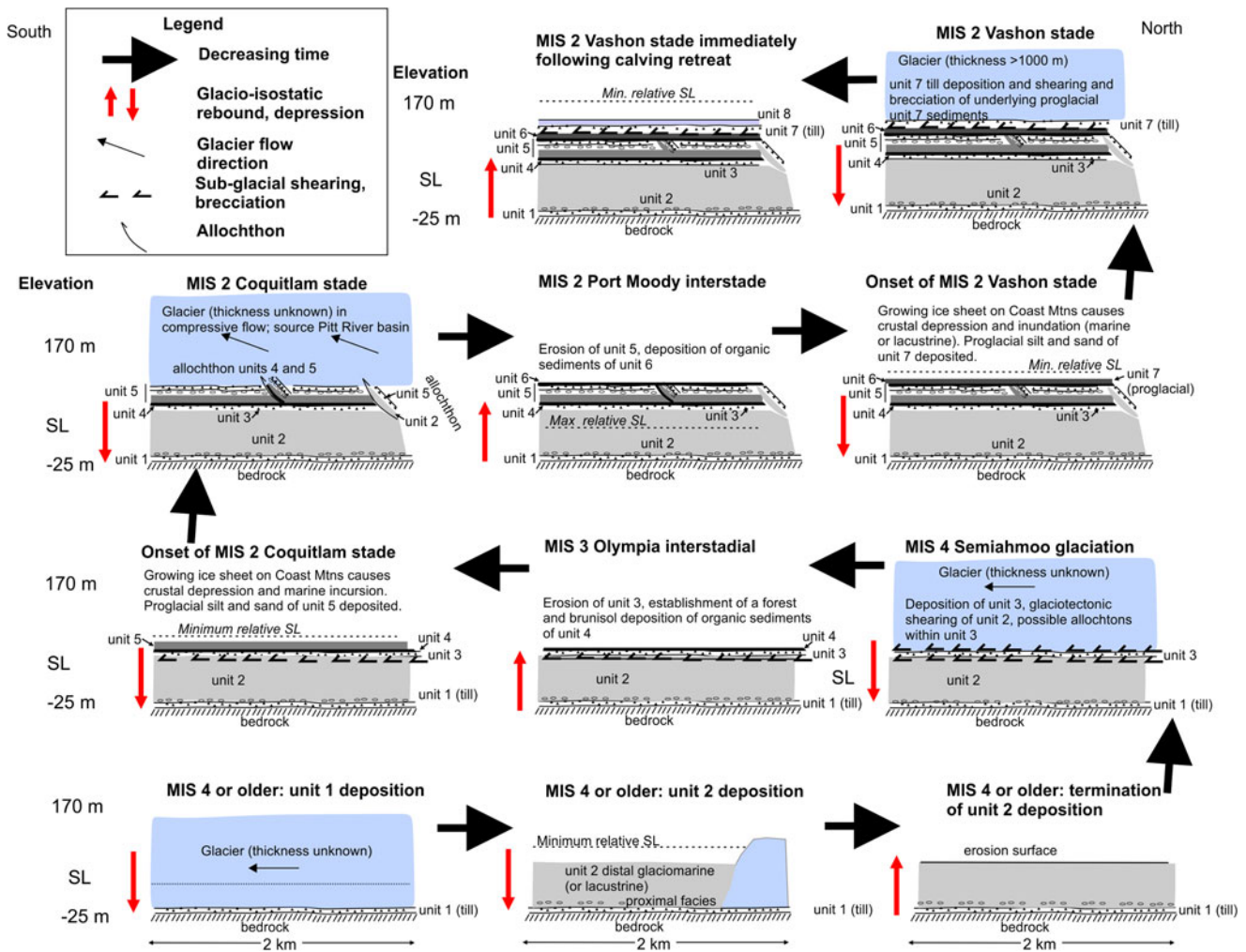


Figure 12. Generalized glacial and nonglacial events within Evergreen fjord beginning with the deepest unit encountered by reconnaissance drilling. The thicknesses of thin units are exaggerated for visibility. MIS, Marine Isotope Stage; SL, sea level.

preserved. Where in situ organics are absent, unit 6 (PM in Fig. 10, BH06-6) is marked by an unconformity that indicates subaerial erosion between the Coquitlam and Vashon stades.

Unit 7: Late MIS 2 Vashon Drift of the Vashon stade

We assign unit 7 to the Vashon Drift (formalized by Hicock and Armstrong, 1985). The zone of glaciotectionism (sV) beneath diamicton formed during the Vashon stade, and it is up to 10 m thick (Figs. 5 and 8, BH15-02). This zone of shearing suggests that a significant portion of basal flow of the Cordilleran Ice Sheet in this area involved deformation of underlying sediments. Lian and Hicock (2010) documented similar brittle deformation of Vashon till and sub-till sediments in nearby valleys in the southern Coast Mountains.

The abrupt burial of unit 6 organic sediments during the onset of the Coquitlam stade occurred during low eustatic sea level (Bard *et al.*, 1990; Chappell *et al.*, 1996; Fig. 13). The lack of Port Moody interstadial sediments below about 60 m asl suggests that the area was still inundated above the present datum. This implies that although the Cordilleran Ice Sheet retreated from the Port Moody-Coquitlam area, it was still extensive enough in the region to remain a force in depressing the crust so that relative

sea level was above the present datum despite lowered eustatic sea level. The subsequent rising relative sea level at the onset of the Vashon stade may have had two causes. One is damming of the Fraser Lowland by the Cordilleran Ice Sheet as it advanced eastward into the Fraser Lowland from what is now the Salish Sea. A second is further regional glacio-isostatic depression in front of the expanding ice sheet. The former could have caused initial inundation. Glacio-isostatic depression would have inevitably followed as the ice sheet advanced into the Evergreen fjord area. The two may have occurred at the same time. There is no evidence to indicate whether the inundation of unit 6 was due to seawater or freshwater.

Allochthons of units 2, 5, and 7 Vashon Drift of the Vashon stade

Cores recovered from boreholes in the northernmost part of Evergreen fjord (Fig. 11, BH09-212, BH09-213, and BH09-214) have evidence for the most extensive glaciotectionism. Age control in these cores comes from two ^{14}C dates on detrital wood fragments in BH09-214: $22,800 \pm 190$ cal yr BP (U215257) and $23,020 \pm 110$ cal yr BP (U215258). These correlate to the Port Moody interstage (Fig. 2). We assign the intense shearing and

Table 4. Glacial and nonglacial event codes (Figs. 8–11).

Unit number	MIS ^a	Glaciation/nonglacial	Event codes	Comments
1	≥4	No older than mid-Pleistocene	PS (till)	Gravelly till on bedrock; oldest known glacial advance in Evergreen fjord
2	≥4	No older than mid-Pleistocene	rPS	Recessional sequence beginning with ice-proximal sediments overlying PS till and fining upward into stoneless silt and sandy silt
3	4	Semiahmoo glaciation	S-1 S-2 S-3 rS sS	Till and ice proximal sediments underlying sediments dated to MIS 3; S-1, S-2, and S-3 may be discrete tills or a stack of allochthons including recessional sediments displaced during a single advance, or sheared intervals. Sand and gravel deposited during glacial recession. Sheared intervals or allochthons; includes the sheared upper 2 m of rPS and gravel overlying an unconformity beneath S1
4	3	Olympic interstadial	OI	Beds of organic material ¹⁴ C dated to MIS 3 along with an underlying paleosol developed in S-3 and a root that penetrated previously glaciotectionized sediments beneath S-3; may include gravel deposited on an unconformity eroded on S-3
5	2	Coquitlam stade, Fraser glaciation	C pC rC sC	Bracketed in age by underlying organic sediments of OI dating to MIS 3 and overlying organic sediments dated to the Port Moody interstade. Includes till and ice-proximal sediments deposited by glacial ice. Sand deposited in advance of glacial ice. Sand and gravel deposited during glacial recession. Allochthons and sheared intervals deformed beneath glacial ice. Allochthons include OI and rPS.
6	2	Port Moody interstade	PM	Beds of in situ plant material or detrital wood in sand and silt derived from in situ beds or vegetation growing during Port Moody interstade; includes an unconformity that truncates rC sediments eroded when the area was above relative sea level
7	2	Vashon stade, Fraser glaciation	V pV sV	Vashon stade sediments include till and ice-contact sediments (V). Pro-glacial fine sand deposited on Port Moody interstade organic sediments and an unconformity eroded during the Port Moody interstade. These fine sediments coarsen upward to sand with gravel and dropstones that represent the rise in relative sea level or a glacially dammed lake in advance of an expanding Cordilleran Ice Sheet at the beginning of the Vashon stade. PM, pV, and Coquitlam stade sediments sheared or detached as allochthons during the passage of glacial ice and deposition of V
8	2	Capilano sediments	CS	Capilano sediments were deposited immediately following the calving retreat of the Vashon stade Cordilleran Ice Sheet in a high stand of relative sea level. They are dominated by coarse to medium sand with dropstones. They are analogous to recessional units rPS, rS, and rC from previous glacial cycles.

^aMIS, Marine Isotope Stage.

stacking of allochthons below this dated interval to the Coquitlam stade (sC; e.g., BH14-03 and 14-04 in Fig. 10) and the shearing of the dated interval and overlying sediments to the Vashon stade (sV; see below). Allochthons associated with the Coquitlam stade include thick bodies of silt derived from unit 2. These allochthons are found where Evergreen fjord narrows between the Chines and Burnaby Mountain (Fig. 1). We suggest that southward-flowing glacial ice experienced compressive flow in this narrow reach that caused upthrusting in underlying sediments during the Coquitlam stade and Vashon stade. However, the sparse age control on these allochthons opens the possibility that the deformation may have occurred during the Semiahmoo glaciation and the Coquitlam stade. Consequently, we indicate “C or older” in labeling the multiple tills encountered in the cores below the dated interval in Figure 11.

Unit 8: Capilano sediments (late MIS 2)

We assign unit 8 to Capilano sediments (best documented by Armstrong, 1981). Capilano sedimentation (CS) marks the final retreat of the Cordilleran Ice Sheet from the area and immediate incursion of marine waters (marine bivalves are common within

Capilano sediments) to elevations of nearly 200 m asl (Fig. 12) before 15.5 cal yr BP. Capilano sedimentation occurred during an episode of rapid eustatic sea-level rise (Figs. 12 and 13) and glacio-isostatic rebound (detailed in the next section). Buried soils within Capilano sediments (Fig. 11, BH09-212 and BH09-214) show that relative sea level fluctuated in an interplay between glacio-isostatic rebound and eustatic sea-level rise, so that some locations were emergent long enough for soils to develop followed by inundation by sea-level rise.

Evidence for repeated Glacio-Isostatic depression and high stands of relative sea level

The Evergreen cores detailed in the preceding sections record four cycles of glacial advance and retreat, separated by intervals of erosion and nonglacial conditions. The oldest glacial event is MIS 6 or older (or alternatively an early phase of MIS 4); the next oldest is MIS 4; and finally the last two are stades of MIS 2. The cores also record a relative sea-level history. The glacial cycles associated with MIS 4 and MIS 2 show evidence of significant glacio-isostatic depression associated with ice-sheet advances. Advance-phase isostatic depression in the region was inferred but not quantified

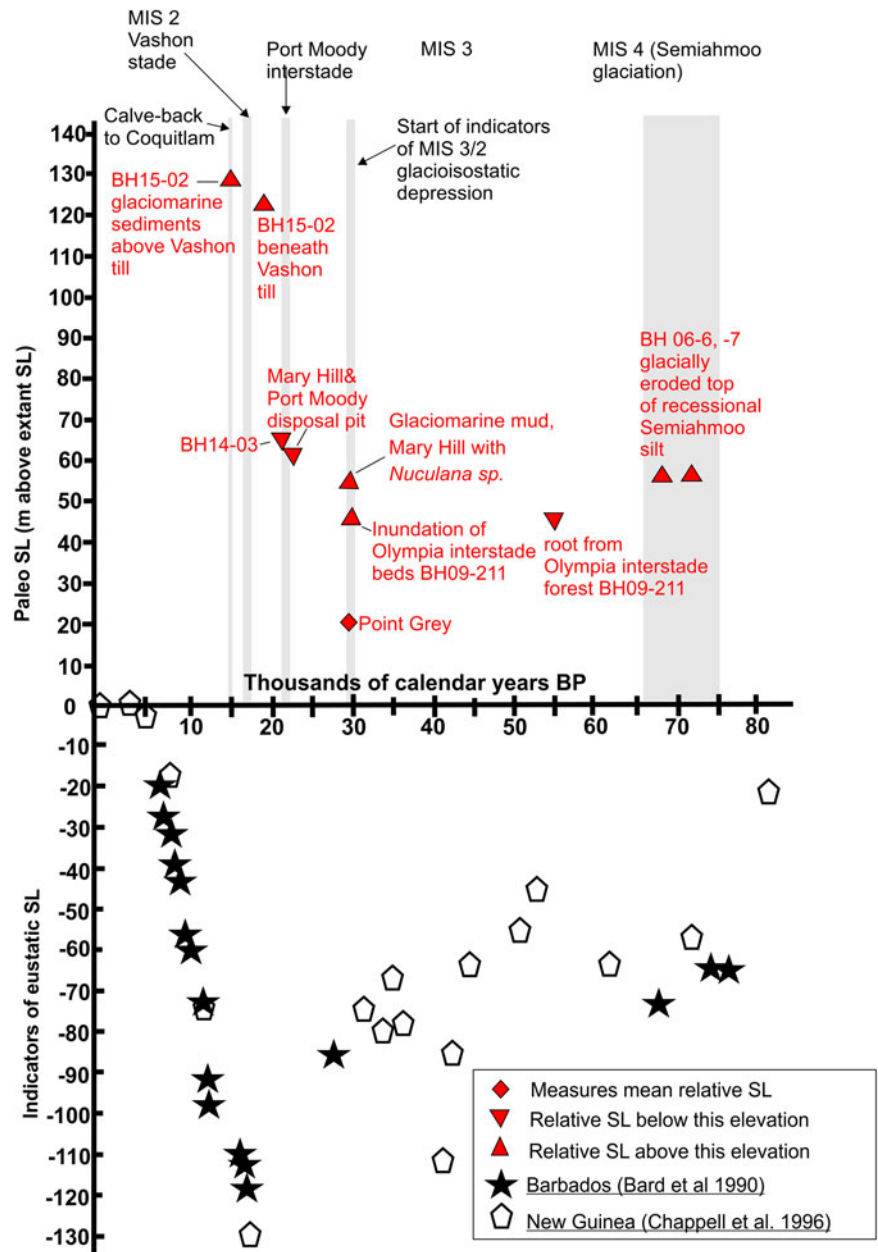


Figure 13. Indicators of relative sea level in cores and results from previous studies plotted against indicators of global eustatic sea level. Sources: Point Grey data from Clague *et al.* (2005); Mary Hill data from Hicock (1976); indicators of eustatic sea level from Barbados (Bard *et al.*, 1990) and Huon Peninsula, New Guinea (Chappell *et al.*, 1996). MIS, Marine Isotope Stage; SL, sea level.

by Al-Suwaidi *et al.* (2006) for the west coast of Vancouver Island and well-quantified by Clague *et al.* (2005) in the Point Grey area of Vancouver (Fig. 1). The record in the Evergreen fjord area, together with previously reported information from Vancouver and Coquitlam, allows greater resolution of the relative sea level for MIS 2 and, to a lesser extent, for MIS 4. Figure 13 shows non-glaciotectonically deformed stratigraphic units chosen as proxy indicators of relative sea level (equal to, above, or below) during MIS 4 and MIS 2. Calibrated ^{14}C ages are plotted along with radiometrically dated corals in Barbados (Bard *et al.*, 1990) and Huon Peninsula, New Guinea (Chappell *et al.*, 1996) that serve as indicators of eustatic sea level. Estimated sea levels are also presented in the schematic summary in Figure 12.

The ages of units 1 and 2 in BH06-6 remain unknown; thus their relationship to eustatic sea level at a specific time cannot be established. Consequently, they are not included in Figure 13. However, the upper boundary of unit 2 is about

42 m asl and records either a high relative sea level or a high stand of a glacially dammed lake. Unit 2 is inundated, and efforts to disaggregate it to isolate foraminifera or diatoms that might indicate marine or freshwater conditions were unsuccessful.

A high stand of relative sea level immediately following the end of MIS 4 (Semiahmoo glaciation) is recorded as ice-proximal sediments in cores BH06-6 and BH06-7 (Fig. 10). They have been eroded and thus provide only a minimum elevation for a high stand of relative sea level at that time, assuming a rapid calving retreat of the MIS 4 ice sheet. Limited control on eustatic sea level suggests isostatic depression of at least 110 m at the time of ice retreat from the area at the end of MIS 4.

High stands of relative sea level following glacial maxima in the Evergreen fjord area can be much more reliably estimated for MIS 2 (Fraser glaciation). At the onset of the Coquitlam stade, MIS 3 subaerial organic sediments in BH09-211 (Figs. 6A,7A, and 10) are about the same age as organic-rich beds in the lower part of

Quadra Sand at Point Grey (Clague et al., 2005; Fig. 1). The beds at Point Grey were deposited in a brackish environment and show that relative sea level was higher than at present at the beginning of the Coquitlam stade as the Cordilleran Ice Sheet was developing over the adjacent Coast Mountains and a trunk glacier was advancing southward along the Georgia Depression between the mainland and Vancouver Island. At Point Grey, these beds extend to 18 m asl and, when combined with estimates of eustatic sea level at that time, indicate that the crust was isostatically depressed approximately 110 m (Clague et al., 2005). In BH09-211, subaerial peaty MIS 3 sediments are disconformably overlain by fine sand from 43–55 m asl. The lowest 10 cm of the fine sand contains reworked plant detritus derived from the underlying MIS 3 sediments (Fig. 7A). It is unclear whether this inundation was by sea water or fresh water based on the Evergreen cores alone. However, at the former Mary Hill sand and gravel pit, 9 km southeast of Evergreen fjord (Fig. 1, MH), Hicock (1976) and (Hicock and Armstrong, 1981) identified tests of the small saltwater clam *Nuculana* sp. in fossiliferous stony glaciomarine sediments that stratigraphically underlie the Coquitlam stade till. These glaciomarine sediments are coeval with sediments overlying MIS 3 sediments in BH09-211. Taken together, this evidence indicates that the Fraser Lowland along the foot of the Coast Mountains was depressed at least 140 m relative to eustatic sea level in advance of the expanding Cordilleran Ice Sheet in the Coquitlam area. This indicates a moat-like downward flexure of the crust in the Fraser Lowland as adjacent areas were loaded by a growing ice sheet.

With regard to the Port Moody interstade, the Evergreen fjord area rose due to glacio-isostatic rebound with the retreat of glacial ice at the end of the Coquitlam stade. In situ subaerially deposited organic sediments occur as low as 61 m asl at Mary Hill, 61 m asl in the Port Moody disposal pit (Hicock and Lian, 1995), and 66 m asl in core BH 14-03 (Fig. 1). Assuming these elevations are close to the paleo-shoreline at that time and there was a marine connection, total isostatic depression during the Port Moody interstade would have been at least 180 m as depicted in Figure 13. However, it is not clear whether there was an open connection between the Evergreen tunnel area and the ocean at this time, or whether it was emergent within a glacially dammed lake. There is no evidence of the Port Moody interstade at Point Grey, 28 km to the west, where a single till overlies Quadra Sand. It is possible that the Sisters Creek Formation was deposited here but was eroded during the subsequent Vashon stade. However, we note that there is no indication that sediments were deposited between the Coquitlam and Vashon stades elsewhere in the Georgia Depression, beyond the Greater Vancouver area (Fig. 1). Two possible explanations exist concerning the presence or absence of a trunk glacier in the Georgia Depression at the time of the Port Moody interstade: either the single till overlying the Quadra Sand at Point Grey was deposited by a trunk glacier after the Port Moody interstade, or a trunk glacier was present at Point Grey at that time but did not reach the Evergreen fjord area. If the till at Point Grey was deposited after the Port Moody interstade, marine waters would have entered the Evergreen area during that interstade. If, on the other hand, glacial ice covered Point Grey during the Port Moody interstade, it may have blocked marine waters from entering the Fraser Lowland and created a glacially dammed lake to the east. Regardless of whether the area was within an ice-dammed lake or open to the sea, Burnaby Mountain and the Chines were islands connected by emergent areas of the Evergreen fjord fill

standing above a water body ca. 60 m above present sea level based upon the occurrences of Port Moody-age terrestrial organic deposits.

Maximum relative sea level is well documented during the initial retreat of the Cordilleran Ice Sheet from the Evergreen tunnel area at the termination of the Vashon stade. BH15-02, the test boring with the highest surface elevation, intersected sand with dropstones (CS) above Vashon till and just below the present ground surface, now 130 m asl (Fig. 8). Sand with dropstones reaches to about 155 m asl 1 km to the east in the Chines area. These elevations are consistent with established upper limits of relative sea level during calving retreat of the Cordilleran Ice Sheet in the Greater Vancouver area (Clague and James, 2002; Jackson et al., 2009, 2014). Compared with indicators of global eustatic sea level at that time, glacio-isostatic depression would have been about 275 m when the Cordilleran Ice Sheet initially retreated from the Evergreen fjord area.

Port Moody interstade and the Laurentide Ice Sheet

The Port Moody interstade marks local recession of glaciers into the adjacent Coast Mountains following the Coquitlam stade. There is no evidence to suggest that this was driven by climatic warming. Rather, paleoenvironmental indicators reveal that although summers were moist and temperate, relatively dry conditions prevailed during long cold winters when storm tracks were displaced south of the Cordilleran Ice Sheet (Lian et al., 2001). We propose that the relatively dry winters resulted in a negative budget in the glaciers covering the Coast Mountains that, in turn, caused glacial recession and triggered local glacio-isostatic rebound. We further hypothesize that the change in winter precipitation was influenced by the Laurentide Ice Sheet. Dyke and Prest (1987) estimated its maximum extent in southern Alberta and northern Montana at ca. 21.9 cal yr BP (ca. 18 ¹⁴C ka BP) based on ¹⁴C dating within glacial limits and glaciological assumptions. Campbell and Campbell (1997) undertook a similar approach using calibrated ¹⁴C ages determined on material lacking any “dead carbon.” They determined an age range of between 21,650 and 21,310 cal yr BP for the last and coincidentally all-time glacial limit along the Alberta–Montana border. Subsequent ³⁶Cl cosmogenic dating of glacial erratics from the Canadian Shield and Rocky Mountains in the same area (Jackson et al., 2011) yielded MIS 2 ages, corroborating that the MIS 2 limit was the all-time limit of glaciation, but the age spread of dated erratics likely indicates that some of them were exhumed. Cosmogenic exposure dating of the Foothills Erratics Train in Alberta (Margold et al., 2019) indicates that the Laurentide Ice Sheet had wasted and deposited the erratics train by ca. 15,000 yr BP.

Collectively, these studies show that the age range of the Laurentide Ice Sheet maximum corresponds to the end of the Coquitlam stade and the Port Moody interstade (Hicock et al., 1999), and its early recession corresponds with the Vashon stade. Support for the supposition of influence of waxing and waning of the southwestern Laurentide Ice Sheet on glacial events in the Salish Sea region is provided by Hicock et al. (1982), who postulate that the full-bodied Laurentide Ice Sheet east of the Cordillera influenced atmospheric circulation in southwest British Columbia by diverting Pacific storm tracks away from the Coast Mountains, especially during winter, when snow critical for determining glacial mass balance was reduced. They and Lian et al. (2001) suggest that when the Laurentide Ice Sheet began to decay, zonal weather patterns over the eastern Pacific shifted

northward and brought wet winters to the Fraser Lowland. This provided moisture for rapid and extensive expansion of the Cordilleran Ice Sheet during the Vashon stade, when it reached its maximum extent in the Salish Sea region ca. 17.7 cal yr BP (ca. 14 5 ¹⁴C ka BP) (Hicock and Armstrong, 1985; Porter and Swanson, 2017). The Laurentide Ice Sheet was well into its retreat east of the Cordillera at that time (Margold et al., 2019; Clark et al., 2022). Atmospheric/ice sheet modeling is required to test these hypotheses.

Conclusions

Stratigraphic test drilling for a light rail transit tunnel between Port Moody and Burnaby in the Greater Vancouver area of British Columbia intersected a fjord infilled with glacial and nonglacial sediments. One boring intersected 130 m of sediment above bedrock, whereas others did not reach bedrock at greater depths, suggesting that the fill exceeds 130 m. Four incursions of glacial ice into the Coquitlam area are documented in the recovered sediments. These correlate with previously established stratigraphic units in the Georgia Depression/Fraser Lowland region. The two most recent advances, the Coquitlam and Vashon stades, date to MIS 2 (Fraser glaciation). The second-oldest glaciation is thought to date to MIS 4 (Semiahmoo glaciation). MIS 3 (Olympia interstadial) nonglacial sediments separate MIS 4 and MIS 2 glacial sediments and include a truncated Brunisol and a root from a forest that grew in the area. The oldest glaciation recorded in the fjord fill may mark an early MIS 4 stade or date to MIS 6 or an older time. An unambiguous chronology could not be established for these older sediments, but they are magnetically normal and thus are younger than 780,000 yr.

At most localities in the Salish Sea/Georgia Depression, a single till was deposited by trunk glaciers during each glacial cycle. However, local conditions prevailed during MIS 2 in the Coquitlam area. The onset of the Coquitlam stade was marked by marine inundation of subaerial peat deposits laid down during MIS 3, indicative of glacio-isostatic depression adjacent to the Coast Mountains as the Cordilleran Ice Sheet expanded and entered the Fraser Lowland. Marine waters entered the Greater Vancouver area despite eustatic sea level being about 80 m lower than present. The Evergreen fjord area was covered by glacial ice during the Coquitlam stade. The subsequent brief Port Moody interstade was marked by local isostatic rebound following local retreat of Coquitlam stade glaciers. We propose that this recession reflected decreased moisture reaching local mountains during winters when storm tracks were diverted south of the Cordilleran Ice Sheet due to the influence of the Laurentide Ice Sheet, when it reached its maximum along the east flank of the Cordillera.

Port Moody interstade organic sediments were inundated in a manner similar to MIS 3 Olympia interstadial sediments. However, is not clear whether they were inundated by sea water or fresh water, due to the possibility of damming of the Fraser Lowland by a trunk glacier in the Strait of Georgia.

Evidence of glaciotectionism is common within Evergreen fjord sediments and ranges from penetrative shearing or brecciation of glacial and nonglacial sediments to transport and stacking of allochthons. Allochthons predominate in the northern parts of the Evergreen tunnel area, which suggests to us that narrowing of the fjord in this area caused compressive flow and shearing in by southward-flowing glaciers.

Successive inundation of erosional surfaces documents a repeated pattern of moat-like depression of the Fraser Lowland

as successive ice sheets grew in mass in the adjacent Coast Mountains and advanced into lowlands. Marine inundation followed ice recession over these isostatically depressed areas.

Supplementary material. The supplementary material for this article can be found at <https://doi.org/10.1017/qua.2024.9>.

Acknowledgments. The Evergreen Line Project, British Columbia Ministry of Transportation, and SNC Lavalin generously shared geotechnical data and cores. Without their support, this project would not have been possible. We would like to acknowledge and dedicate the paper to paleoecologist Alice Telka, who prepared many samples collected from the cores for ¹⁴C dating. She passed away during this project. Funding for a portion of this project was provided by an NSERC grant RGPIN/06887-2018 to BCW. Funding for RG was provided by the German Research Foundation (DFG grant no. GR 5663/1-1). We gratefully acknowledge the collaboration of Randolph J. Enkin at the Paleomagnetism Laboratory of Pacific Geoscience Centre, Sidney, British Columbia; Rudy Reimer, Department of Archaeology, Simon Fraser University (SFU); and James MacEachern, Department of Earth Sciences (SFU). The project would not have gone forward without the efforts of Matthew Plotnikoff, manager, Laboratory & Field Operations at the SFU Department of Earth Sciences, who found space to store and work on half a kilometer of cores and many students who helped. The authors gratefully acknowledge reviews by Olav B. Lian, an anonymous reviewer, senior editor Derek B. Booth, and associate editor Jason Dortch. Their rigorous and very helpful comments greatly improved this paper.

References

- Agriculture and Agri-foods Canada**, 1998. *The Canadian System of Soil Classification*. 3rd ed. <https://sis.agr.gc.ca/cansis/taxa/cssc3/index.html>.
- Alley, N.F., Hicock, S.R.**, 1986. The stratigraphy, palynology, and climatic significance of pre-middle Wisconsin Pleistocene sediments, southern Vancouver Island, British Columbia. *Canadian Journal of Earth Sciences* **23**, 369–382.
- Al-Suwaidi, M., Ward, B.C., Wilson, M.C., Hebda, R.J., Nagorsen, D.W., Marshall, D., Ghaleb, B., Wigen R.J., Enkin, R.J.**, 2006. Late Wisconsinan Port Eliza Cave deposits and their Implications for human coastal migration, Vancouver Island, Canada. *Geoarchaeology* **21**, 307–332.
- Armstrong, J.A.**, 1975. *Quaternary Geology, Stratigraphic Studies and Reevaluation of Terrain Inventory Maps, Fraser Lowland, British Columbia*. Paper 1975 1A. Geological Survey of Canada, Ottawa, pp. 377–380.
- Armstrong, J.E.**, 1953. Geology of sand and gravel deposits, lower Fraser Valley, British Columbia. *Bulletin of Canadian Mining and Metallurgy*, April 1953, pp. 234–241.
- Armstrong, J.E.**, 1981. Post-Vashon Wisconsin Glaciation, Fraser Lowland, British Columbia. *Geological Survey of Canada Bulletin* **322**.
- Armstrong, J.E., Brown, W.L.**, 1953. *Ground-Water Resources of Surrey Municipality, British Columbia*. Canada Department of Mines and Technical Surveys. Water Supply Paper No. 322. Geological Survey of Canada, Ottawa.
- Armstrong, J.E., Clague, J.J.**, 1977. Two major Wisconsin lithostratigraphic units in southwest British Columbia. *Canadian Journal of Earth Sciences* **14**, 1471–1480.
- Armstrong, J.E., Crandell, D.R., Easterbrook, D. J., Noble, J.B.**, 1965. Late Pleistocene stratigraphy and chronology in southwestern British Columbia and northwestern Washington. *Geological Society of America Bulletin* **76**, 321–330.
- Armstrong, J.E., Hicock, S.R.**, 1975. *Quaternary Landscapes, Present and Past at Mary Hill, Coquitlam, British Columbia*. Paper 75-1B. Geological Survey of Canada, Ottawa, pp. 99–103.
- Armstrong, J.E., Hicock, S.R.**, 1976. *Quaternary Multiple Valley Development of the Lower Coquitlam Valley, Coquitlam, British Columbia*. Paper 76-1B. Geological Survey of Canada, Ottawa, pp. 197–200.
- Armstrong, J.E., Hicock, S.R.**, 1979. Surficial Geology, Vancouver, British Columbia. Map 1486A. 1:50,000. Geological Survey of Canada, Ottawa.
- Bard, E., Hamelin, B., Fairbanks, R.G.**, 1990. U–Th ages obtained by mass spectrometry in corals from Barbados; sea level during the past 130,000 years. *Nature* **346**, 456–458.

- Benn, D.I., Evans, D.J.A.**, 1996. The interpretation and classification of sub-glacially deformed materials. *Quaternary Science Reviews* **15**, 23–52.
- Booth, D.B., Troost, K.G., Clague, J.J., Waitt, R.B.**, 2003. The Cordilleran Ice Sheet. In: Gillespie, A.R., Porter, S.C., Atwater, B.F. (Eds.), *Developments in Quaternary Sciences*. Vol. 1. Elsevier, Amsterdam, pp. 17–43.
- Campbell, C., Campbell, I.A.**, 1997. Calibration, review and geomorphic implications of postglacial radiocarbon ages in southeastern Alberta, Canada. *Quaternary Research* **47**, 37–44.
- Chappell, J., Omura, A., Esat, T., McCulloch, M., Pandolfi, J., Ota, Y., Pillans, B.**, 1996. Reconciliation of late Quaternary sea levels derived from coral terraces at Huon Peninsula with deep sea oxygen isotope records. *Earth and Planetary Science Letters* **141**, 227–236.
- Clague, J.J.**, 1976. Quadra Sand and its relation to the late Wisconsin glaciation of southwest British Columbia. *Canadian Journal of Earth Sciences* **13**, 805–815.
- Clague, J.J.**, 1977. Quadra sand: a study of the Late Pleistocene geology and geomorphic history of coastal southwest British Columbia. Geological Survey of Canada, Paper, 77-17. <https://doi.org/10.4095/103057>.
- Clague, J.J.**, 1983. Glacio-isostatic effects of the Cordilleran ice sheet, British Columbia, Canada. In: Smith, D.E., Dawson, A.G. (Eds.), *Shorelines and Isostasy*. Academic Press, London, pp. 321–343.
- Clague, J.J.**, 1985. The Quaternary stratigraphic record of British Columbia—evidence for episodic sedimentation and erosion controlled by glaciation. *Canadian Journal of Earth Sciences* **23**, 885–894.
- Clague, J.J.**, 1989. Cordilleran ice sheet. In: Fulton, R.J. (Ed.), *Quaternary Geology of Canada and Greenland*. Geological Survey of Canada, Ottawa, pp. 40–43.
- Clague, J.J., Froese, D., Hutchinson, James, T.S., Simon, K.M.**, 2005. Early growth of the last Cordilleran ice sheet deduced from glacio-isostatic depression in southwest British Columbia, Canada. *Quaternary Research* **63**, 53–59.
- Clague, J.J., James, T.S.**, 2002. History and isostatic effects of the last ice sheet in southern British Columbia. *Quaternary Science Reviews* **21**, 71–87.
- Clague, J.J., MacDonald, G.M.**, 1989. Paleocology and paleoclimatology (Canadian Cordillera). In: Fulton, R.J. (Ed.), *Quaternary Geology of Canada and Greenland*. Geological Survey of Canada, Geology of Canada, no. 1; Geological Society of America, The Geology of North America, Vol. K-1. Ottawa; Boulder, CO, pp. 70–74.
- Clague, J.J., Ward, B.C.**, 2011. Pleistocene Glaciation of British Columbia. In: J. Ehlers, J., P.L. Gibbard, P.L. Hughes, P.D. (Eds.), *Developments in Quaternary Sciences*. Vol. 15. Elsevier, Amsterdam, pp. 563–573.
- Clark, D.H., Clague, J.J.**, 2020. Glaciers, isostasy, and eustasy in the Fraser Lowland: a new interpretation of late Pleistocene glaciation across the International Boundary. In: Waitt, R.B., Thackray, G.D., Gillespie, A.R. (Eds.), *Untangling the Quaternary Period—A Legacy of Stephen C. Porter*. Geological Society of America Special Paper **548**, 255–274.
- Clark, J., Carlson, A.E., Reyes, A.V., Carlson, E.C.B., Guillaume, L., Milne, G.A., Tarasov, L., Caffee, M., Wilcken, K., Roode, D.H.**, 2022. The age of the opening of the Ice-Free Corridor and implications for the peopling of the America. *Proceedings of the National Academy of Sciences USA* **119**, e2118558119.
- Cosma, T.N., Hendy, I.L., Chang, A.S.**, 2008. Chronological constraints on Cordilleran Ice Sheet glaciomarine sedimentation from core MD02-2496 off Vancouver Island (western Canada). *Quaternary Science Reviews* **27**, 941–955.
- Dyke, A.S., Prest, V.K.**, 1987. Paleogeography of Northern North America 18 000–5000 Years Ago. Map 1703A. 1:12 500 000. Geological Survey of Canada, Ottawa.
- Easterbrook, D.J.**, 1992. Advance and retreat of Cordilleran ice sheets in Washington, U.S.A. *Géographie Physique et Quaternaire* **46**, 51–68.
- Easterbrook, D.J.**, 1994. Chronology of pre-Late Wisconsin Pleistocene sediments in Puget Lowland, Washington. *Washington Division of Mines and Earth Resources Bulletin* **80**, 191–206.
- Golder Associates**, 2010. Evergreen Line Rapid Transit Project, Twin Tunnels [Unpublished geotechnical data report]. Golder Associates, Vancouver, BC.
- Hebda, R.J., Lian, O.B., Hicock, S.R.**, 2016. Olympia Interstadial: vegetation, landscape history, and paleoclimatic implications of a mid-Wisconsinan (MIS3) nonglacial sequence from southwest British Columbia, Canada. *Canadian Journal of Earth Sciences* **53**, 304–320.
- Heusser, C.J.**, 1977. Quaternary palynology of the Pacific slope of Washington. *Quaternary Research* **8**, 282–306.
- Hicock, S.R.**, 1976. Quaternary Geology: Coquitlam–Port Moody Area, British Columbia. MSc thesis. University of British Columbia, Vancouver, BC.
- Hicock, S.R., Armstrong, J.E.**, 1981. Coquitlam drift: a pre-Vashon Fraser glacial formation in the Fraser Lowland, British Columbia. *Canadian Journal of Earth Sciences* **18**, 1443–1451.
- Hicock, S.R., Armstrong, J.E.**, 1983. Four Pleistocene formations in southwest British Columbia: their implications for patterns of sedimentation of possible Sangamonian to early Wisconsinan age. *Canadian Journal of Earth Sciences* **20**, 1232–1247.
- Hicock, S.R., Armstrong, J.E.**, 1985. Vashon Drift: definition of the formation in the Georgia Depression, southwest British Columbia. *Canadian Journal of Earth Sciences* **22**, 748–757.
- Hicock, S.R., Hebda, R.J., Armstrong, J.E.**, 1982. Lag of the Fraser glacial maximum in the Pacific Northwest: Pollen and macrofossil evidence from western Fraser Lowland, British Columbia. *Canadian Journal of Earth Sciences* **19**, 2288–2296.
- Hicock, S.R., Lian, O.B.**, 1995. The Sisters Creek Formation: Pleistocene sediments representing a nonglacial interval in southwestern British Columbia at about 18 ka. *Canadian Journal of Earth Sciences* **32**, 758–767.
- Hicock, S.R., Lian, O.B.**, 1999. Cordilleran Ice Sheet lobal interactions and glaciotectonic superposition through stadial maxima along a mountain front in southwestern British Columbia, Canada. *Boreas* **28**, 531–542.
- Hicock, S.R., Lian, O.B., Mathewes, R.W.**, 1999. “Bond cycles” recorded in terrestrial Pleistocene sediments of southwestern British Columbia, Canada. *Journal of Quaternary Science* **14**, 443–449.
- Jackson, L.E., Andriashek, L.D., Phillips, F.M.**, 2011. Limits of successive Middle and Late Pleistocene continental ice sheets, Interior Plains of southern and central Alberta and adjacent areas. In: Ehlers, J., Gibbard, P.L., Hughes, P.D. (Eds.), *Developments in Quaternary Sciences*. Vol. 15. Elsevier, Amsterdam, pp. 575–589.
- Jackson, L.E., Blais-Stevens, A., Hermanns R.L., Jermyn C.E.**, 2014. Late Glacial and Holocene sedimentation and investigation of fjord tsunami potential in lower Howe Sound, British Columbia. In: Lollino, G., Manconi, A., Locat, J., Huang, Y., Canals Artigas, M. (Eds.), *Engineering Geology for Society and Territory*. Vol. 4. Springer, New York, pp. 59–62.
- Jackson, L.E., Jr., Blais-Stevens, A., Shaw, A.L., van Zayle, D., Hetherington, R., Hermanns, R.L., Jermyn, C.E., Barrie, C.V., Kim Conway, K., Kung, R.**, 2009. *Late Glacial and Holocene Sedimentation in Lower Howe Sound*. Canadian Quaternary Association 2009 Annual Meeting, Mid Conference Field Trip, 6 May 2009, 36 pp.
- James, T.S., Clague, J.J., Wang, K., Hutchinson, I.**, 2000. Postglacial rebound at the northern Cascadia subduction zone. *Quaternary Science Reviews* **19**, 1527–1541.
- Lian, O.B., Hickin, E.J.**, 1993. The Late Pleistocene stratigraphy and chronology of lower Seymour Valley, southwestern British Columbia. *Canadian Journal of Earth Sciences* **30**, 841–850.
- Lian, O.B., Hicock, S.R.**, 2010. Insight into the character of palaeo-ice-flow in the upland regions of mountain valleys during the last major advance (Vashon Stade) of the Cordilleran Ice Sheet, southwest British Columbia. *Boreas* **39**, 171–186.
- Lian, O.B., Hu, J., Huntley, D.J., Hicock, S.R.**, 1995. Optical dating studies of Quaternary organic-rich sediments from southwestern British Columbia and northwestern Washington State. *Canadian Journal of Earth Sciences* **32**, 1194–1207.
- Lian, O.B., Mathewes, R.W., Hicock, S.R.**, 2001. Palaeoenvironmental reconstruction of the Port Moody Interstade, a nonglacial interval in southwestern British Columbia at about 18 000 ¹⁴C years. *Canadian Journal of Earth Sciences* **38**, 943–952.
- Lisiecki, L.E., Raymo, M.E.**, 2005. A Pliocene-Pleistocene stack of 57 globally distributed benthic ¹⁸O records. *Paleoceanography* **20**, PA1003.
- Margold, M., Gosse, J.C., Hidy, A.J., Woywitka, R.J., Young, J.M., Froese, D.**, 2019. Beryllium-10 dating of the Foothills Erratics Train in Alberta, Canada, indicates detachment of the Laurentide Ice Sheet from the Rocky Mountains at ~15 ka. *Quaternary Research* **92**, 469–482.
- Mathewes, R.W.**, 1991. Climatic conditions in the western and northern Cordillera during the last glaciation: paleoecological evidence. *Géographie physique et Quaternaire* **45**, 333–339.

- Miller, R.F., Morgan, A.V., Hicock, S.R., 1985. Pre-Vashon fossil Coleoptera of Fraser age from the Fraser Lowland, British Columbia. *Canadian Journal of Earth Sciences* **22**, 498–505.
- Mustard, P.S., Rouse, G.E., 1994. Stratigraphy and evolution of Tertiary Georgia Basin and subjacent Upper Cretaceous sedimentary rocks, southwestern British Columbia and northwestern Washington State. In: Monger, J.W.H. (Ed.), *Geology and Geological Hazards of the Vancouver Region, Southwestern British Columbia*. Geological Survey of Canada Bulletin **481**, 97–169.
- Porter, S.C., 2011. Glaciation of western Washington, USA. In: Ehlers, J., Philip, P.L., Hughes, D. (Eds.), *Quaternary Glaciations—Extent and Chronology*. Developments in Quaternary Science, Vol. 15. Elsevier, Amsterdam, pp. 531–536.
- Porter, S.C., Swanson, T.W., 2017. Radiocarbon age constraints on rates of advance and retreat of the Puget Lobe of the Cordilleran Ice Sheet during the last glaciation. *Quaternary Research* **50**, 205–213.
- Reimer, P.J., Austin, W.E.N., Bard, E., Bayliss, A., Blackwell, P.G., Ramsey, C.B., Butzin, M., *et al.*, 2020. The INTCAL20 Northern Hemisphere radiocarbon age calibration curve (0–55 cal kBP). *Radiocarbon* **62**, 725–757.
- Roberts, A.P., Turner, G.M., 2013. Geomagnetic excursions and secular variations. In: Elias, S. (Ed.), *Encyclopedia of Quaternary Science*. 2nd ed. Vol. 1. Elsevier, Amsterdam, pp. 705–720.
- Siddall, M., Rohling, E.J., Thompson, W.G., Waelbroeck, C., 2008. Marine Isotope Stage 3 sea level fluctuations: data synthesis and new outlook. *Reviews of Geophysics* **46**, 1–29.
- Smith, C.A.S., Webb, K.T., Kenney, E., Anderson, A., Kroetsch, D., 2011. Brunisolic soils of Canada: genesis, distribution, and classification. *Canadian Journal of Soil Science* **91**, 695–716.
- Stuiver, M., Polach, H.A., 1977. Discussion reporting of ^{14}C data. *Radiocarbon* **19**, 355–363.